Vertebrate extinction across Permian–Triassic boundary in Karoo Basin, South Africa

Gregory J. Retallack†
Department of Geological Sciences, University of Oregon, Eugene, Oregon 97403, USA

Roger M.H. Smith
Department of Earth Sciences, South African Museum, Post Office Box 61, Cape Town 8000, South Africa

Peter D. Ward
Department of Geological Sciences, Box 351310, University of Washington, Seattle, Washington 98195, USA

ABSTRACT

Distinct assemblages of paleosols above and below the Permian–Triassic boundary in the Karoo Basin of South Africa are evidence for reorganization of ecosystems following this greatest of all mass extinctions. The Permian–Triassic boundary is recognized from the last appearance of *Dicynodon* and from a series of negative excursions in the isotopic composition of carbon within therapsid tusks, pedogenic carbonate nodules, and organic matter. The boundary is also marked by laminated beds with very weakly developed paleosols, a change from purple (10R) to brownish red (2.5YR) paleosols, and a thin (10-cm) claystone breccia of reworked soil clasts. Paleoclimatic changes include a shift from arid and highly seasonal paleoclimate inferred from diffuse and shallow calcareous nodules in Permian paleosols to semiarid and less seasonal paleoclimate inferred from deep and well-focused calcic horizons in Triassic paleosols. An earliest Triassic shift to warmer and wetter paleoclimate is also indicated by increased chemical weathering, abundance of lycopsids, and diversity of labyrinthodonts. Permian paleosols have root traces comparable to those of open shrubland and riparian woodland, whereas Triassic paleosols have root traces and profile forms like soils of open woodland. This is a significant paleoenvironmental change, but not as dramatic a change as would be expected from the devastating extinctions of 88% of fossil vertebrate genera. Latest Permian therapsid reptiles were diverse and ecologically specialized. In contrast, the principal earliest Triassic therapsid, *Lystrosaurus*, was a burrower with no specific habitat preference. Its short internal nares, barrel chest, and high neural spines would have given it greater aerobic scope than preexisting therapsids and may have been an advantage under conditions of hypercapnia and hypoxia. These adaptations and associated ecosystem changes are compatible with widespread vertebrate mortality by acidosis and pulmonary edema in a postapocalyptic greenhouse created by the voluminous release of methane from shallow marine and permafrost clathrates.

Keywords: paleosol, vertebrate, Permian–Triassic, Karoo Basin, South Africa.

INTRODUCTION

Therapsid fossils of the Karoo Basin of South Africa (Figs. 1 and 2) are an important record of the Permian–Triassic mass extinction, complementing patterns of extinction documented for that greatest of all life crises among marine shellfish (Yang et al., 1996; Knoll et al., 1996) and plants (Retallack, 1995; Wang, 1996; Looy et al., 2001). Terminal Permian extinction among South African vertebrates was abrupt and severe (Smith and Ward, 2001). Few creatures survived, and of these, *Lystrosaurus* was by far the most abundant and widespread land vertebrate. Why did this animal survive when others did not? Its stout limbs, barrel chest, high neural spines, short tail, propalinal jaw action, and beak—toothless except for two prominent upper tusks—have attracted a variety of interpretations of this extinct animal as amphibious, beaverlike, turtlelike, or burrower (King and Cluver, 1991). Another line of evidence explored here for the habits and habitats of these animals is the sediments and soils on which they walked, lived, and died (Retallack, 1996; Retallack and Hammer, 1998). Paleosols containing bones and burrows of *Lystrosaurus* are also evidence of its ecosystem. Although fossil bones are abundant in the *Lystrosaurus* and *Dicynodon* zones of South Africa, paleosols are found at even more stratigraphic levels (Smith, 1995) and provide a more complete record of both times and places of Permian–Triassic events (Retallack, 1999a; Retallack and Krull, 1999). Were therapsids and their ecosystems killed by a bolide impact (Becker et al., 2001), flood basaltic eruptions (Renne et al., 1995; Riechow et al., 2002), or methane clathrate dissociation events (Morante, 1996; Krull et al., 2000; Krull and Retallack, 2000)? The main subjects of this paper are latest Permian and earliest Triassic paleosols, their description, classification, and what they can tell us about the world's greatest mass extinction of land vertebrates.

PINPOINTING THE PERMIAN–TRIASSIC BOUNDARY

Recent progress in identifying the Permian–Triassic boundary within the Karoo and other Gondwana basins guided our choice of locations and methods. The Beaufort Group in the Karoo Basin is a thick sequence of Permian and Triassic alluvial outwash derived from mountains of the Cape Fold Belt to the south (Fig. 1; Hiller and Stavrakis, 1984; Veevers et al., 1994). Its fluvial depositional environments are clear from cliff-forming, quartzo-

†E-mail: gregr@darkwing.uoregon.edu.

GSA Bulletin; September 2003; v. 115; no. 9; p. 1133–1152; 15 figures; 3 tables; Data Repository item 2003122.

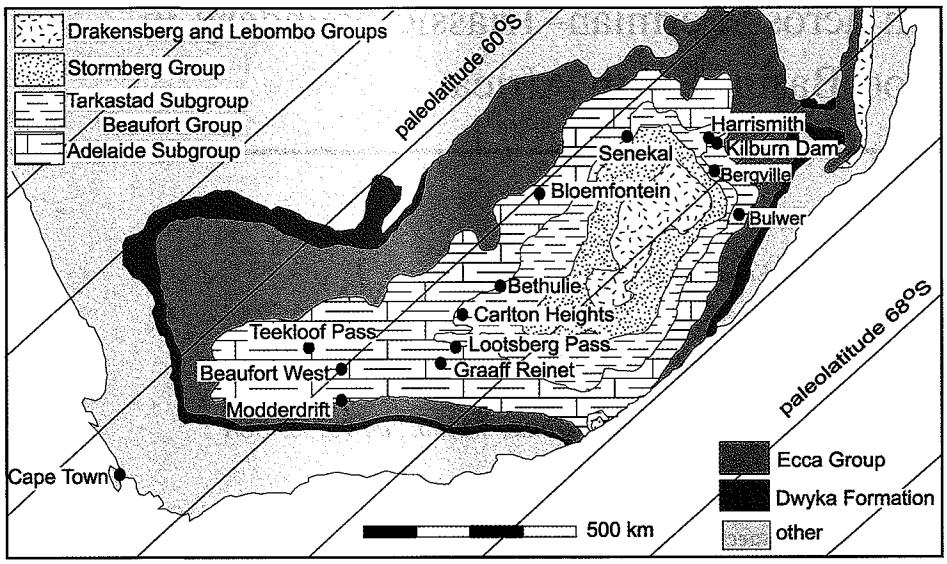

Figure 1. Permian–Triassic boundary sites in Karoo Desert of South Africa. Permian paleolatitudes from de Wit et al. (2002) are shown, but map is oriented as for current location between 25–35°S.

feldspathic sandstones with a variety of sedimentary structures; these are interpreted to have formed in channel, point-bar, levee, crevasse, and chute environments (Smith, 1993a, 1993b; Haycock et al., 1997; Catuneanu and Elango, 2001). Mottled and nodular red and maroon siltstones and claystones with abundant burrows and root traces have been interpreted as sequences of floodplain paleosols (Smith, 1987, 1990; Groenewald, 1991).

Traditionally, the Permian–Triassic boundary was approximated by the boundary between the mainly silty Balfour Formation of the upper Adelaide Subgroup and the mainly sandy Katberg Formation of the basal Tarkastad Subgroup. This lithological change has been interpreted to reflect a change in the nature of ancient rivers from meandering to braided (Smith, 1995; Ward et al., 2000; Hancox et al., 2002). Intensive collection of fossil vertebrates now shows that this lithological change is above the Permian–Triassic boundary, which is within the upper few meters of

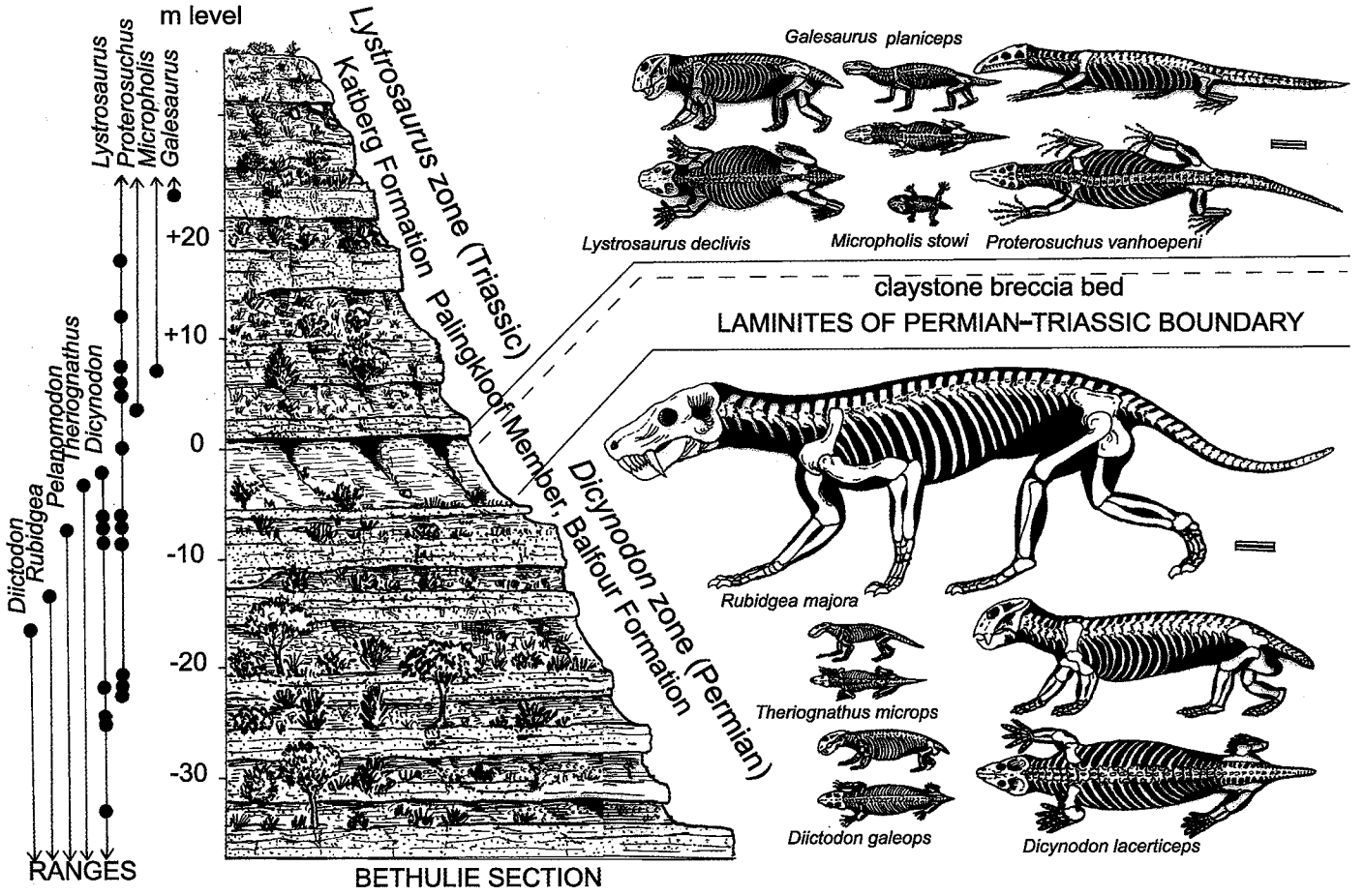

Figure 2. Overview of fossils and sequence near Bethulie, Orange Free State. Fossil ranges are from Smith and Ward (2001), and skeletal reconstructions after Broom (1932), Broili and Schröder (1937), Watson (1960), Haughton (1970), Cluver (1971), Cluver and Hotton, (1981), King (1981, 1991), Kemp (1986), and MacRae (1999).

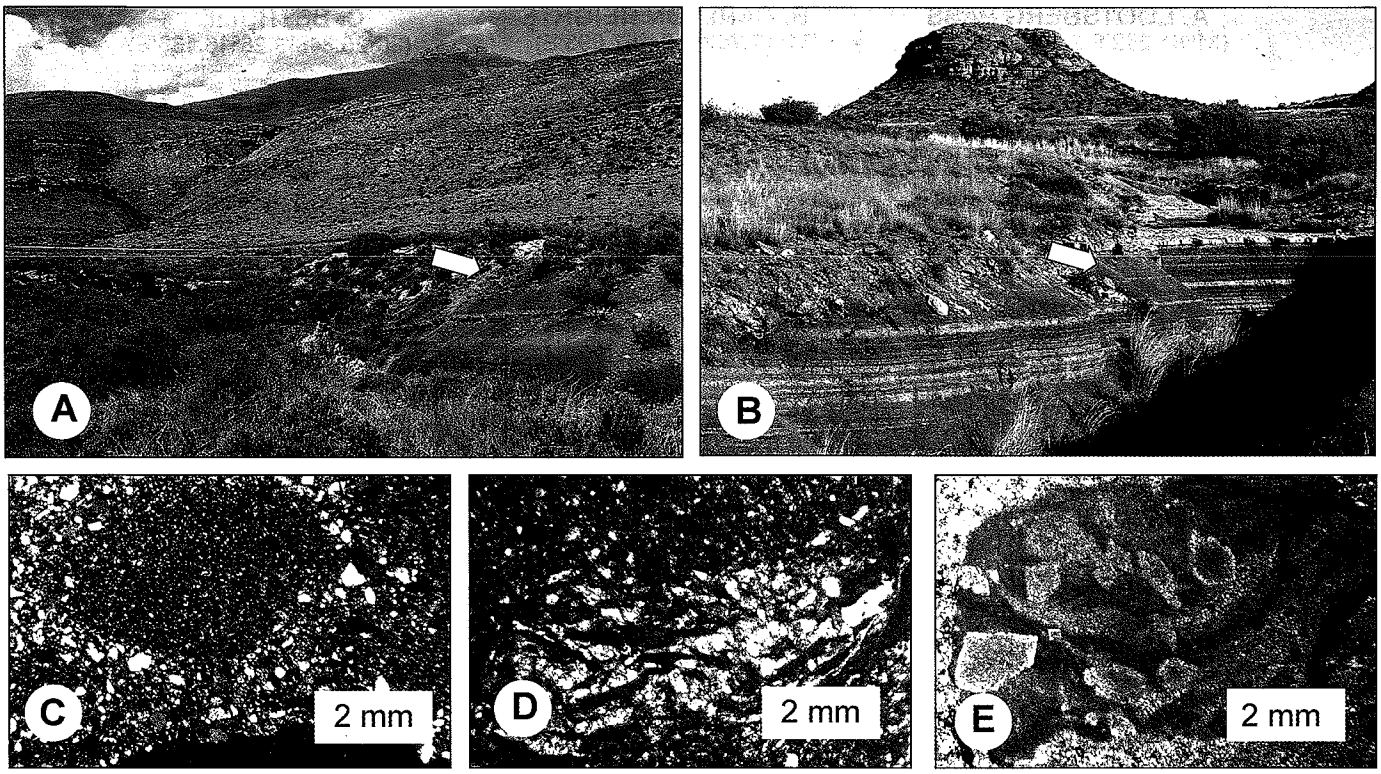

Figure 3. Lootsberg Pass (A) and Bethulie (B) sites for the Permian–Triassic boundary (at arrow), with photomicrographs of boundary breccia at Lootsberg Pass (C), Wapadsburg (D), and Bethulie (E). Redeposited, subangular to subrounded soil clasts in the boundary breccia include soil microfabrics (C, mosepic porphryoskelic), and silica-replaced evaporites (D-E, probably originally gypsum).

the Palingkloof Member of the Balfour Formation (Figs. 2 and 3). The Permian-Triassic boundary in the Karoo Basin is between the *Dicynodon* and *Lystrosaurus* vertebrate zones (Rubidge, 1995). In the northern Karoo Basin, this boundary is incompletely preserved because of erosional disconformities (Hancox et al., 2002). Recently discovered overlap in stratigraphic range of the two nominate taxa in the more complete sequence of the southern Karoo Basin (Fig. 2) is now regarded as latest Permian, with *Lystrosaurus* being one of the few survivors of vertebrate extinction (Smith, 1995; Smith and Ward, 2001).

This biostratigraphic placement of the Permian–Triassic boundary is supported by carbon isotopic analyses of therapsid tusks, organic carbon, and pedogenic carbonate. These analyses reveal the first of several isotopic excursions to negative values at the level of minimum vertebrate diversity (MacLeod et al., 2000). Such isotopic anomalies have been used to recognize the Permian–Triassic boundary at many localities worldwide (Morante, 1996; Krull and Retallack, 2000), including the likely stratotype for the boundary at Meishan, China (Yang et al., 1996). Fossil leaves and pollen are very poorly preserved in Karoo Permian–Triassic boundary rocks (Anderson, 1977; Stapleton, 1978), but unusual abundance of fungal spores from the Carlton Heights section (+17 to +18 m in Fig. 4) has been regarded as a Permian–Triassic boundary fungal spike (Steiner et al., 2001). Unfortunately, there are several fungal spikes at and above the boundary, so these spikes locate the boundary within only a few tens of meters (Visscher et al., 1996; Looy et al., 2001). Furthermore, many palynomorphs identified as fungal hyphae may have been zygnematalean algae, indicative of lakes rather than an earliest Triassic zone of death and decay (Krassilov et al., 1999). Paleomagnetic studies of the Permian–Triassic boundary in South Africa and Antarctica have been plagued by remagnetization during intrusion of Jurassic dolerite dikes, but recent work at Lootsberg Pass has obtained results compatible with those from vertebrate biostratigraphy (Pehl et al., 2001).

Biostratigraphy, paleomagnetism, and isotopic chemostratigraphy indicate that the Permian–Triassic boundary in the southern Karoo Basin is within a 7-m-thick sequence of laminated purple to gray beds (Smith and Ward, 2001). Laminites also were found in the uppermost *Dicynodon* zone in gullies below Ndanja Hill near Bergville in Natal, where they include algal stromatolites. Comparable laminites also have been reported below sandstones of the basal Verkykerskop Formation near Senekal in the northern Karoo Basin (Hancox et al., 2002). We interpret the laminites as deposits of playa lakes. The laminites contain millimetric and varve-like lamination, burrows like those made by crustaceans, and algal stromatolites, but they also contain fossil root traces of very weakly developed paleosols and vertebrate footprints as evidence of periodic drying. The laminites are a distinctive basin-wide facies and form a natural divide between paleosol types, which are very different in the Triassic above and the Permian below (Figs. 2–4). Diffuse shallow calcic horizons are found in paleosols below, but deep, well-focused calcic horizons are found in paleosols above the laminites (Figs. 5–7). Paleosols below are purple-red (10R) and gray, but those above are brownish red (2.5YR) and green.

Comparable laminites also are known in the Murrays Run bore of New South Wales, Australia, where they contain leaves of *Glossopteris* as well as pollen of latest Permian age. They are overlain by rocks with earliest Tri-

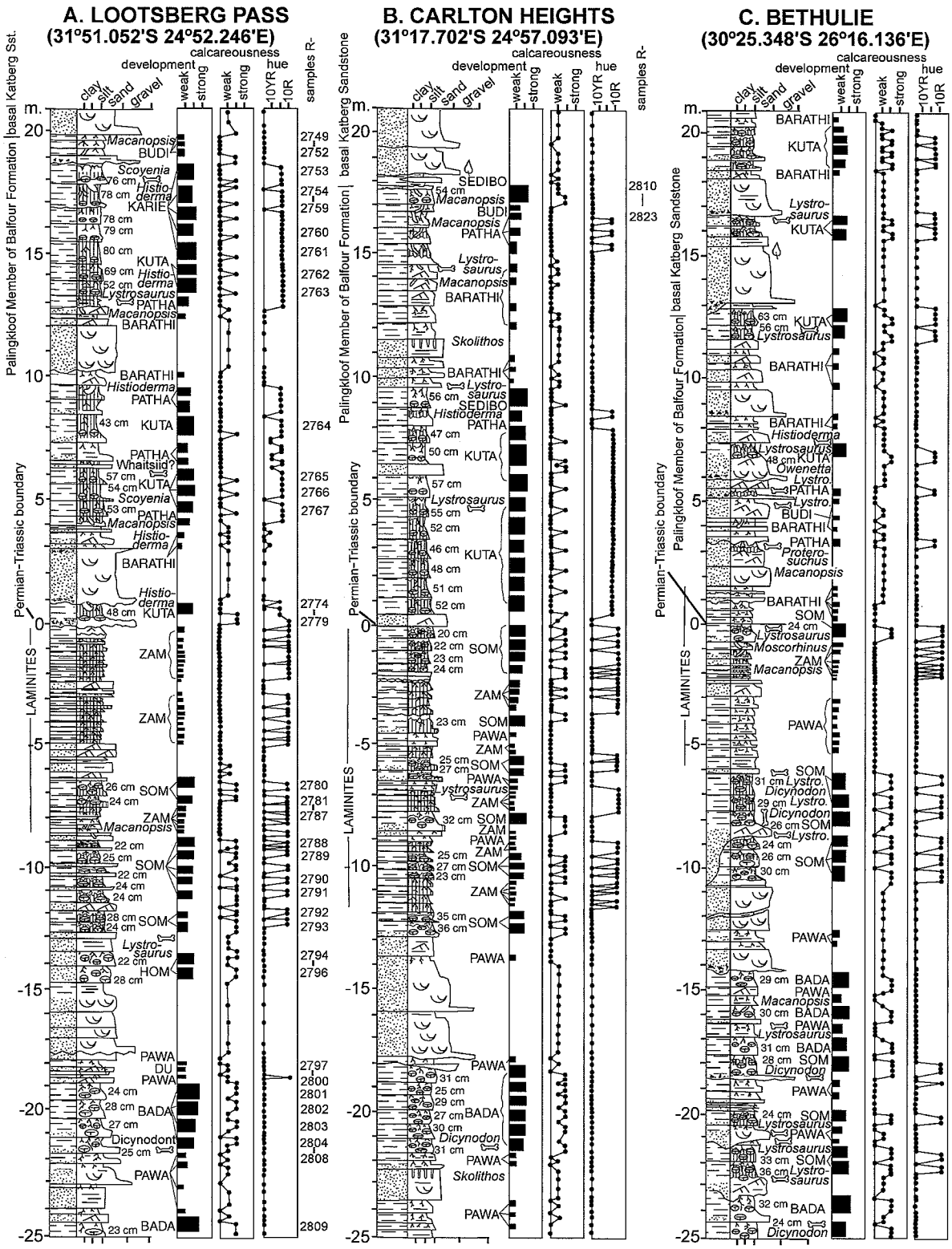

Figure 4. Measured sections across Permian–Triassic boundary at Lootsberg Pass (left), Carlton Heights (middle), and near Bethulie (right). Permian–Triassic boundary is at 0 level. Geographic coordinates are from a Garmin Global Positioning System set to Cape meridian. Lithological key as for Figure 6.

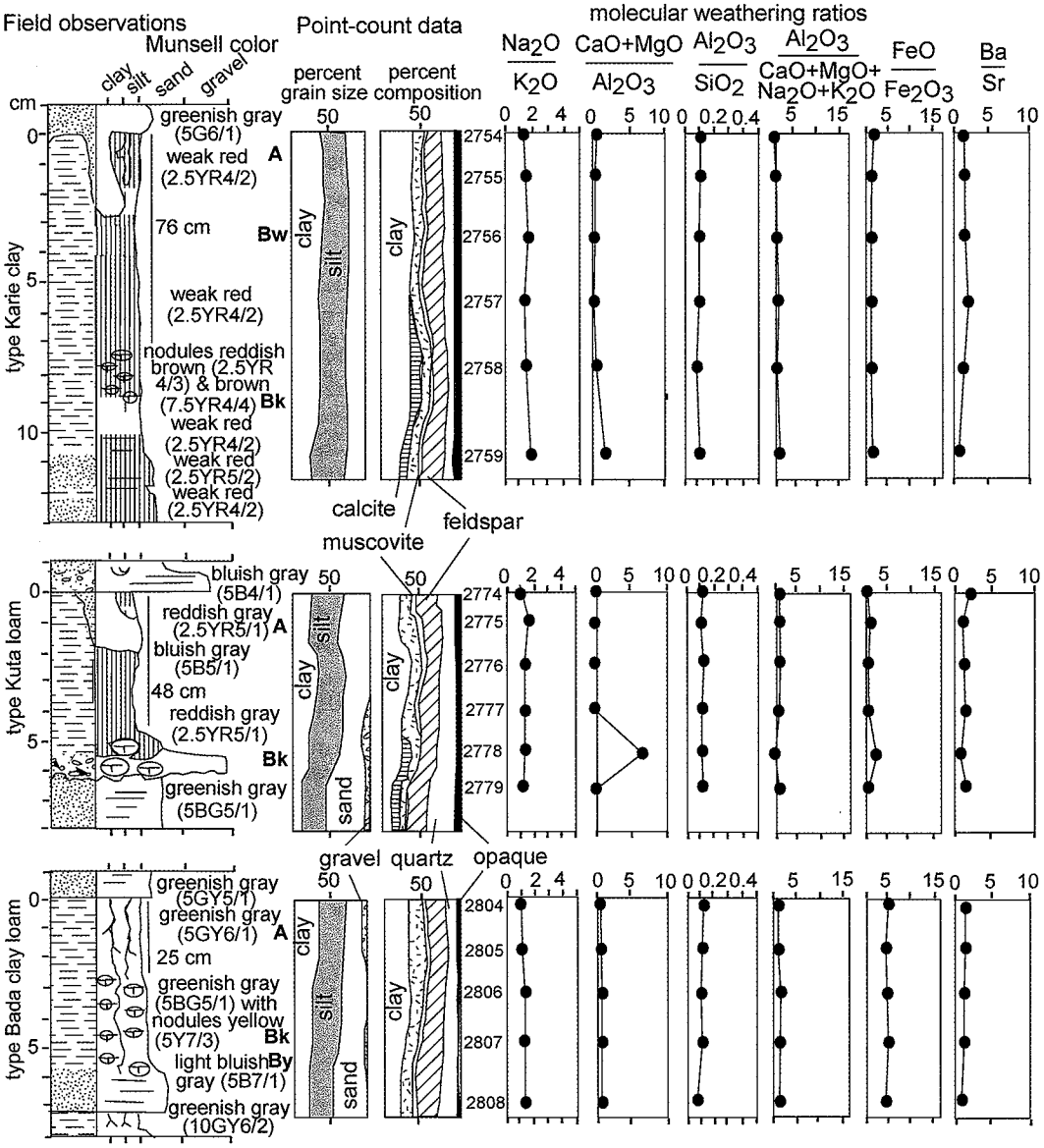

Figure 5. Field, petrographic, and chemical data for type Bada (late Permian), Kuta (earliest Triassic), and Karie (early Triassic) paleosols at Lootsberg Pass, Cape Province. Lithological key as for Figure 6.

assic pollen (Morante, 1996; Retallack, 1999a). Another distinctive laminite at Mt. Crean, Victoria Land, Antarctica, is at the Permian–Triassic boundary as defined by carbon isotopes but lacks fossils (Retallack et al., 1998). The Murrays Run and Mt. Crean laminites correspond to a thick coal seam in other parts of Australia and Antarctica (Retallack, 1999a; Retallack and Krull, 1999). The Australian and Antarctic laminites and coals divide blue and gray, wetland paleosols below, from a different red and green assemblage of paleosols above, comparable with the blue–purple Permian versus red–green Triassic paleosols of the Karoo Basin.

Another distinctive South African bed comparable with beds in Antarctica-Australia is a 10-cm-thick claystone-breccia with subrounded to subangular, moderately to well sorted granules of claystone (Fig. 3, A–E). The granules have distinctive microfabrics, including birefringence fabric (Fig. 3C; mosepic porphyroskelic of Brewer, 1976) and silicified evaporite pseudomorphs (Fig. 3, D–E). Other granules in the claystone breccia are nodules of pedogenic micrite, often with reddish gray (2.5YR5/1) weathering rinds, in contrast to purple and gray enclosing laminites. These microfabrics indicate erosion from well-developed soils and can be matched by microfabrics of Permian paleosols in the same sections. These claystone breccias are very odd beds for the laminite sequences in which they were found at Lootsberg Pass, Wapadsberg, and Bethulie (Fig. 1). A comparable rusty nodular bed within laminites near Senekal in the northern Karoo Basin (Hancox et al., 2002) has long been taken as a Permian–Triassic marker bed (Kitching, 1977). These beds are distinct from those claystone breccias that are likely to have formed by river bank collapse (e.g., at 20 m in Fig. 4A), which are basal to trough cross-bedded sandstone and have highly angular, poorly sorted clasts with unweathered, laminated, or weakly weathered (insepic agglomeroplasmic) microfabric. Nor do the claystone breccias include elongate, curved, or rounded clay chips, like those redeposited from desic-

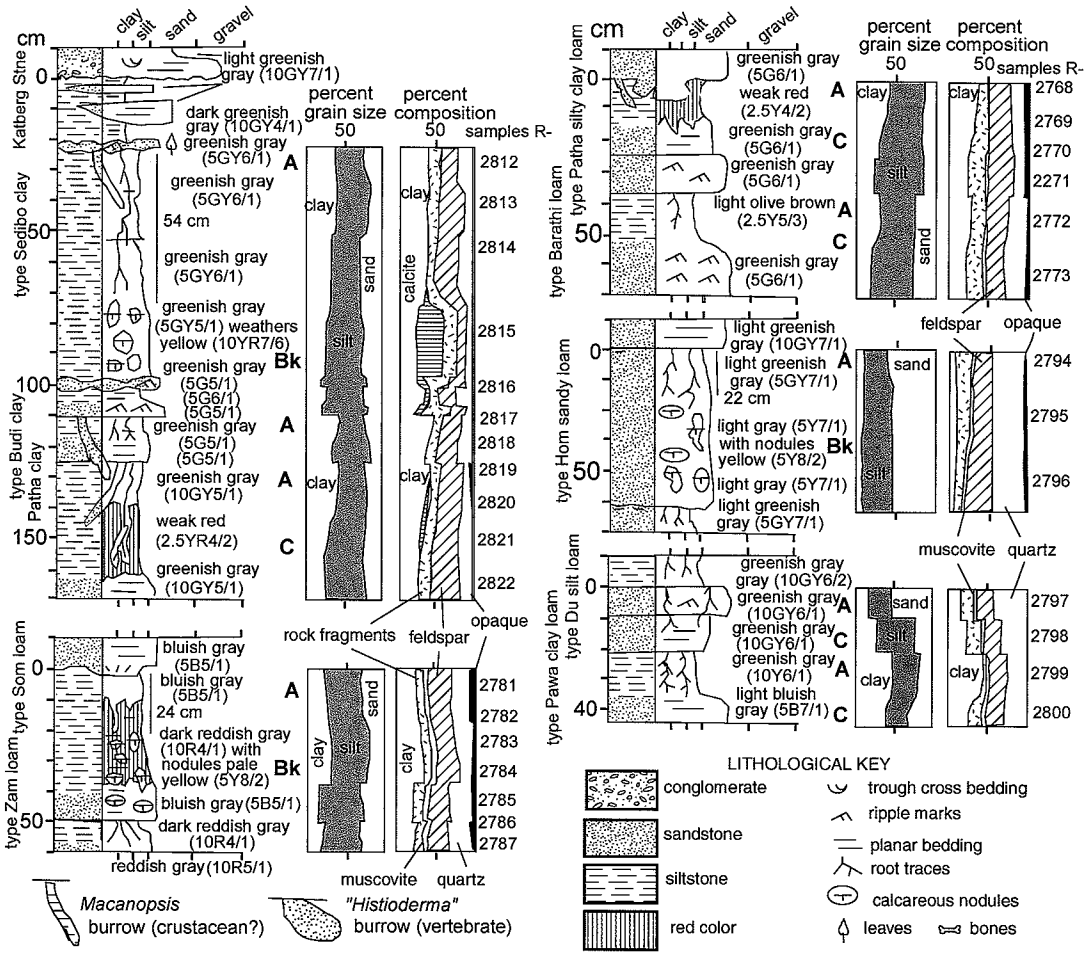

Figure 6. Field and petrographic data for type Sedibo, Budi, and Patha paleosols (early Triassic) at Carlton Heights and for type Barathi (early Triassic) and type Hom, Du, Pawa, Som, and Zam paleosols (late Permian) at Lootsberg Pass.

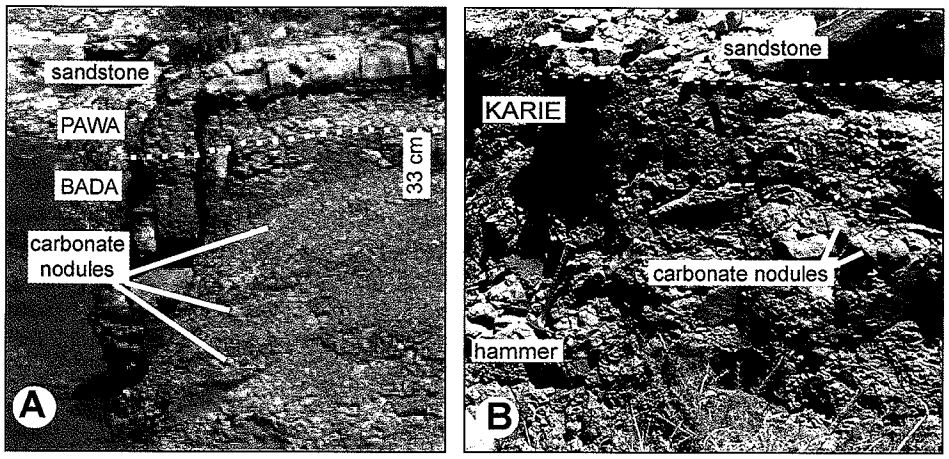

Figure 7. Field photographs of Pawa and Bada paleosols at −21 m in Bethulie section (A) and type Karie paleosol at Lootsberg Pass (B). Depth to calcareous nodules in this Bada paleosol is 33 cm; in Karie paleosol it is 76 cm.

cation cracks of mud flats. The 10-cm claystone breccia in laminites and the upper parts of point bar cycles are quite different in appearance and thin section (Fig. 3). The claystone breccia beds are also unusually thin for debris-flow deposits, such as the 9-m-thick, matrix-supported conglomerate at the Permian–Triassic boundary in the Raniganj Basin of India (Sarkar et al., 2003). Thin, claystone breccias deposited by sheet flow are common on footslopes after clear-cutting of forest in Oregon today. The subrounded to subangular, moderately sorted clasts are little-modified subangular blocky peds and nodules of soils washed downhill after the stabilizing effect of undergrowth has been destroyed by log hauling. The soil-derived clasts within these deposits break down in western Oregon's humid climate to become indistinguishable from ordinary sediments after clear cuts or ground fires only 3 yr old. We interpret the claystone-breccias of the boundary interval as pedoliths produced by an unusual pe-

TABLE 1. CLASSIFICATION OF PEDOTYPES ACROSS PERMIAN–TRIASSIC BOUNDARY

Pedotype	Khoisan	Diagnosis	South African	Australian	U.S. taxonomy	FAO world map
Triassic paleosols (*Lystrosaurus* zone)						
Barathi	Green	Bedded olive brown shale with fine root traces	Dundee mtamvuna	Alluvial soil	Fluvent	Eutric Fluvisol
Budi	Burrow	Bedded green-gray sandstone with root traces and burrows	Dundee kowie	Humic gley	Fluvaquent	Gleyic Cambisol
Karie	Thick	Reddish brown (2.5YR) with deep, well-focused calcareous nodules (Bk)	Addo spekboom	Solonized brown soil	Vertic Haplocalcid	Calcic Xerosol
Kuta	Den	Gray surface (A) over reddish brown (2.5YR) with shallow, well-focused calcareous nodules (Bk)	Prieska naatwe	Solonized brown soil	Sodic Haplocalcid	Calcic Xerosol
Patha	Crack	Reddish brown (2.5YR) with relict bedding, root traces, and burrows	Tukulu hoeko	Brown clay	Haploxerept	Eutric Cambisol
Sedibo	Patch	Greenish-gray with deep, well-focused calcareous nodules (Bk)	Montagu baden	Gray clay	Calcic Aquisalid	Calcaric Gleysol
Permian paleosols (*Dicynodon* zone)						
Bada	Grave	Gray siltstone with shallow and scattered calcareous nodules and rhizoconcretions (Bk)	Montagu baden	Desert loam	Calcic Aquisalid	Calcic Yermosol
Du	Sand	Bedded blue-gray sandstone with fine root traces	Dundee nonoti	Alluvial soil	Fluvaquent	Dystric Fluvisol
Hom	Sand	White sandstone with shallow and scattered calcareous nodules and rhizoconcretions (Bk)	Montagu knipes	Calcareous sand	Calcixerept	Calcic Cambisol
Pawa	Clay	Bedded blue-gray shale with fine root traces	Dundee mtamvuna	Alluvial soil	Fluvent	Eutric Fluvisol
Som	Shade	Gray siltstone surface (A) over purple (10R) siltstone with shallow calcareous nodules (Bk)	Montagu scoma	Wiesenboden	Aquic Calcixerept	Calcic Cambisol
Zam	Thin	Bedded purple-gray (10R) siltstone with fine root traces and burrows	Dundee seekoei	Alluvial soil	Fluvent	Eutric Fluvisol

riod of soil erosion followed by accelerated rates of sedimentation.

This pedolith interpretation is made even more remarkable by reports of comparable claystone breccias at other Permian–Triassic boundary sections in Australia and Antarctica. There, the claystone clasts also are of local derivation, including kaolinitized clay skins (argillans of Brewer, 1976), like those in underlying coal measures of the Sydney Basin of Australia (Retallack, 1999a), and volcanic and metamorphic clasts weathered to smectite and illite as in underlying coal measures of Graphite Peak, Antarctica (Retallack and Krull, 1999). In Australian and Antarctic sections, claystone breccia is at a level in the section where the last tree leaves (mainly *Glossopteris*) and roots (*Vertebraria*) give way to smaller woody and hollow roots and a very different assemblage of leaves and pollen of earliest Triassic age (Retallack, 1995). Extinction of woody Permian plants and replacement by dominantly herbaceous Triassic vegetation have been inferred from palynological studies (Looy et al., 2001; Twitchett et al., 2001). Geochemical studies of a spike of organic matter at the Permian–Triassic boundary in Italy also have been interpreted as evidence of extensive soil erosion (Sephton et al., 2002). The redeposited soil layer in Antarctica and Australia contains modest amounts (up to 120 ppt over background 15 ppt) of iridium and shocked quartz (Retallack et al., 1998). In the northern Karoo Basin, the boundary bed also has modest levels of iridium (up to 320 ppt over background 100–200 ppt), as well as modest enrichment of Ni and Cr (Hancox et al., 2002). This distinctive claystone breccia marker bed has been used as a datum to align our measured sections (Fig. 4).

MATERIALS AND METHODS

We reexamined 25 m above and below the Permian–Triassic claystone breccia and laminite at well-known localities of the upper Palingkloof Member of the Balfour Formation and the lowermost Katberg Formation. Detailed sections were measured and sampled in the creek below Lootsberg Pass, in road cuts along the old road at Wapadsberg Pass, in the highway road cuts at Carlton Heights down to railway cuts at Carlton siding and 3 km to the northeast, all in eastern Cape Province, and in the creek east of Swartberg, south of Fairydale Farm, near Bethulie, Orange Free State (Figs. 3 and 4). Reconnaissance observations also were made of Teekloof Pass south of Fraserburg, Cape Province; Ndanja Hill east of Bergville, Orange Free State; gullies east of Harrismith, Orange Free State (Rubidge, 1995); and a quarry north of Bulwer, Natal (Anderson and Anderson, 1985). Paleosols were assigned to distinctive types or pedotypes (of Retallack, 1994) in the field (Table 1) and named from descriptive terms in the indigenous Khoisan language (Bleek, 1956). Hand specimens of selected paleosols were chemically analyzed by Bondar-Clegg of Vancouver, British Columbia, using X-ray fluorescence spectrometry with potassium dichromate titration for FeO (see Data Repository).[1] Petrographic thin sections were counted for 500 points using a Swift automatic point counter to determine the grain-size distribution and mineral content of these same profiles (Figs. 5 and 6). These chemical and petrographic data allow classification of the paleosols and their paleoenvironmental interpretation (Retallack 1997a). Fossils pertinent to this project are in the collections of the South African Museum, Cape Town (R.M.H. Smith, curator).

ALTERATION OF PALEOSOLS AFTER BURIAL

The bane of Karoo paleontology is extensive intrusion with dolerite sills and dikes of Jurassic age, which have thermally metamorphosed host rocks. Contact metamorphism reduces bone to powdery lime so that it is difficult to prepare, and it carbonizes plant debris so that pollen and spores become too brittle to extract whole. Our investigation focused on areas free of thick sills, which are potentially the most altering, but there is a prominent dike 5.3 m thick in the Lootsberg Pass section (−14 to −16 m in Fig. 4A) and another 0.6-m thick at the waterfall near the Permian–Triassic boundary in the Bethulie section (Fig. 4C). Intrusions had a pronounced effect on

[1]GSA Data Repository item 2003122, data on Permian–Triassic boundary paleosols in South Africa, is available on the Web at http://www.geosociety.org/pubs/ft2003.htm. Requests may also be sent to editing@geosociety.org.

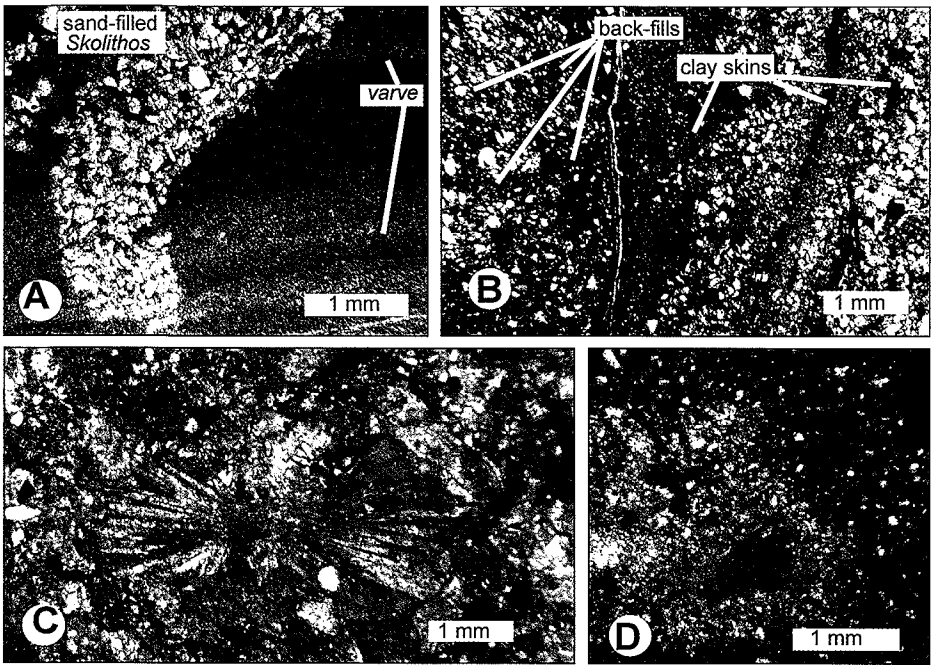

Figure 8. Photomicrographs of illuviation argillans (A), and of varvoid bedding cut by sand-filled *Skolithos* burrow (B), both in Karie paleosol at Lootsberg Pass; and of a gypsum rosette (C) and calcareous rhizoconcretion (D) from Sedibo paleosol at Carlton Heights. Acicular crystals of gypsum have much sharper terminations than superficially similar trace fossils of *Microcodium* (Klappa, 1978; Alonso-Zarza et al., 1998).

color and mineral content of paleosols. Alteration near dikes can be recognized in the field by the black rather than red or gray color of paleosols, friable calcined white bone rather than dark purple- or light gray-stained bone, and hollow zeolitized calcareous nodules. Studies of comparable alteration in Antarctica have shown that the thermal carbonization of vitrinite associated with dolerite dikes is imperceptible at distances of more than twice the dike width (Horner and Krissek, 1991). Discoloration haloes of comparable width are visible around South African dolerite dikes within red beds (Retallack, 1997a, color photo 140). Prehnite and laumontite are common alteration products of carbonate and clay around dikes (Retallack, 1999b). Both minerals are fresh in Antarctic paleosols but have weathered to hollows in thermally altered South African paleosols.

Another problem is alteration of carbonates and clay as a consequence of fluid migration within this thick synorogenic sedimentary sequence shed from the Cape Fold Belt (de Wit et al., 2002). Studies of fluid inclusions and hydrogen and oxygen isotopic composition of veins indicate burial temperatures of 150–170°C and occasionally up to 270 °C (Egle et al., 1998). South African sequences are comparable in severity of burial diagenesis with Permian–Triassic sequences studied in Antarctica (Retallack and Krull, 1999) and Australia (Retallack, 1999a). Such burial alteration should not be exaggerated, however. South African vein calcite formed during burial and deformation has a wider array of carbon isotopic compositions than associated pedogenic carbonate, but the values overlap substantially (de Wit et al., 2002). Illitization of clays has not overwhelmed a distinctive, soda-rich composition of Karoo rocks (Fig. 5), and potash content is no more than 3.56 wt %. We found soda abundance of 1.5–3.0 wt % (see Data Repository), as in the Beaufort and Ecca Groups elsewhere in South Africa (Zawada, 1984, 1988; Hancox et al., 2002). We also found evaporitic pseudomorphs and rosettes (Figs. 3E and 8C). Large pseudomorphs of halite and gypsum have long been known from the Ecca and lower Beaufort Groups (Keyser, 1968; van der Westerhuizen et al., 1981; Smith, 1990, 1993a, 1993b, 1995), and may indicate the local presence of hypersaline paleosols (Solonchak of Food and Agriculture Organization, 1974) within rocks of older Permian age than the paleosols studied here (Fig. 4). These are evidence that pedogenic salinization in an arid climate was not overwhelmed by subsequent burial illitization, which can in any case be modeled as recrystallization by Ostwald ripening without extensive alkali mass transfer (Eberl et al., 1990).

Yet another alteration is compaction of paleosols due to overburden pressure, which was probably only 0.86 km (Rubidge, 1995), because the Molteno and higher Karoo formations were not deposited in this area (Veevers et al., 1994). Using the compaction equation of Sheldon and Retallack (2001), this would compact paleosol thickness by a factor of 0.79. Comparable results come from deconvolution of a sandstone clastic dike, originally a sand-filled crack, within Bada and Som pedotype paleosols 4 m below the base of the section measured near Bethulie (Fig. 4). The dike is 234 cm long in vertical distance of 200 cm for a compaction factor of 0.85. An average compaction factor of 0.79 comes from other observations of eight clastic dikes in paleosols (probably Takyric Solonchaks) of the Hoedemaker Member of the Teekloof Formation (732 m stratigraphically lower than the Permian–Triassic boundary) in road cuts at Teekloof Pass. A compaction factor of 0.8 was used here.

Some sparry calcite in calcareous nodules appears due to neomorphism at depth, because it cuts across and enhances nodule boundaries. Not all spar is neomorphic, because pore-filling spar may have been precipitated during soil formation or shortly after burial. In any case, sparry calcite is rare compared with micritic pedogenic carbonate.

Red and purple color is probably not original, but the result of a dehydration and Ostwald ripening of brown to yellow ferric hydroxides (Retallack, 1991a). Several red and purple paleosols (Karie, Patha, Som) have drab-haloed root traces that probably formed during shallow-burial microbial reduction of soil matrix (Retallack, 1997a), because vertebrate burrows indicate that the water table was deep and there was not an impermeable water-perching soil horizon. This local burial reduction to greenish-gray color was probably fueled by decomposition of soil organic matter, which is evident in all the paleosols from casts and clay-filled impressions of roots rather than carbonaceous remains (Fig. 9). Nevertheless, the original brown versus gray color probably has environmental significance: it was either inherited from rocks of that color with little modification in a very arid climate, or it reflects stagnant groundwater (gleization) for gray color versus well-drained soil pores (oxidation) for brownish colors (Retallack, 1997a).

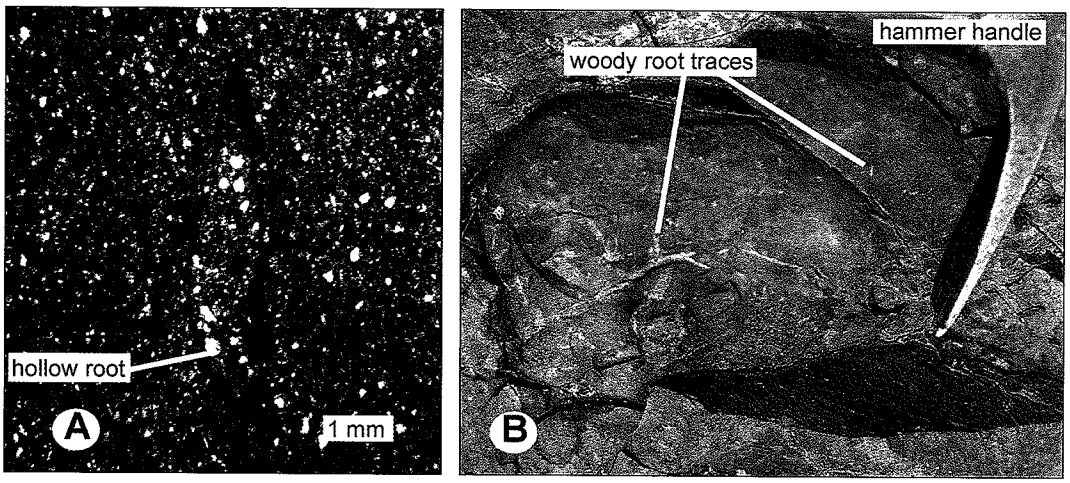

Figure 9. Photomicrograph of hollow lycopsid root in Zam paleosol (A) and woody gymnosperm root traces and hammer head for scale in type Bada paleosol (B), both at Lootsberg Pass.

CLASSIFICATION OF PERMIAN–TRIASSIC PALEOSOLS

Our non-genetic field classification of the Karoo Permian–Triassic boundary paleosols based on degree of bioturbation, nodule development, clay skin density, and color of the paleosols is summarized in Table 1, with selected profile data illustrated in Figures 5–7 and supporting data detailed in the Data Repository. In terms of the simplified field classification of paleosols by Mack et al. (1993), we observed Protosols (Zam, Pawa, Hom, Du, Patha, and Barathi pedotypes), Calcisols (Bada, Som, Kuta, and Karie pedotypes) and Gleysols (Sedibo and Budi pedotypes). Such assemblages of paleosols are found in alluvial bottomlands with seasonally fluctuating, but locally high water tables in arid to semiarid climates (Mack and James, 1994).

More detailed interpretations and distinction between Permian and Triassic conditions come from comparing paleosols with modern soils in an effort to find analogous modern soilscapes. This approach requires laboratory data and must take into account burial modification of chemical and textural criteria for classification, which vary among the classifications we employed (Stace et al., 1968; Food and Agriculture Organization, 1974; Soil Classification Working Group, 1991; Soil Survey Staff, 1999). High soda content in blue-gray calcareous paleosols of the Bada pedotype is also indicated by petrographic observations of gypsum and other salt pseudomorphs (Fig. 8C). Such saline soils with shallow calcareous nodules are Calcic Yermosols of the Food and Agriculture Organization (1974). Bada paleosols lack prismatic peds and clay-rich subsurface horizons of Solonetz and have less salt and better-developed calcareous nodules than Solonchak (of Food and Agriculture Organization, 1974). Bada paleosols are blue-gray in color and have unusually high FeO/Fe_2O_3 ratios (Fig. 5), indicating seasonally inundated (gleyed) soils. They are also weathered little chemically and very silty texturally (Fig. 5), as are desert soils. Hom and Som paleosols are comparable, but for more abundant relict bedding, as in Cambisols (of Food and Agriculture Organization, 1974) and Inceptisols (of Soil Survey Staff, 1999). Bada, Hom and Som are the only Permian pedotypes with large calcareous nodules formed over a long period of time, and they represent formerly stable parts of the landscape. Other latest Permian paleosols (Du, Pawa, Zam) have clear relict bedding (Fig. 10C), indicating a brief time for formation and location near streams, lakes, and other sources of sedimentary disturbance. These identifications of Permian paleosols are most like modern soils of alluvial bottomlands of the Sur Darya River near Kyzl Orda, southeast of the Aral Sea, Kazakhstan (map unit Yk 44–3a of Food and Agriculture Organization, 1978a), northeast of the Kyzl Kum (red sands) and Kara Kum (black sands) Deserts. Kyzl Orda has an arid, cold, continental climate: mean annual precipitation 114 mm (48–187 mm), mean annual temperature 8.3 °C, with July much hotter (24.5 °C) and drier (4 mm) than January (−9.6 °C, 13 mm; Müller, 1982). Vegetation is desert shrubland with sagebrush (*Artemisia*) and tumbleweed (*Salsola*), but with local small trees such as saxaul (*Ammodendron connollyi*; Knystautas, 1987). Analogous soils of South Africa support desert shrubland of sagebrush (*Artemisia*) and vaalkaroo (*Pentzia*: Food and Agriculture Organization, 1977), and in Australia, similar desert scrub of saltbush (*Atriplex vesicaria*) and bluebush (*Kochia sedifolia*: Stace et al., 1968; Food and Agriculture Organization, 1978b).

Triassic paleosols are all different from Permian paleosols, with brownish red and greenish gray rather than purple and bluish gray colors, deeper calcareous horizons, and more prominent illuvial clay (illuviation argillans of Brewer, 1976) in thin section (Fig. 8B). Neither chemical nor petrographic data support interpretation of Karie and Kuta paleosols as argillic (with 1.2 times as much clay as in the surface horizon), and both are chemically quite sodic (Fig. 5). With their prominent calcareous nodules they are best identified as Aridisols (Soil Survey Staff, 1999) and Xerosols (Food and Agriculture Organization, 1974). Sedibo paleosols are gray and have iron-manganese nodules as evidence of gleization due to seasonal inundation, but their calcareous nodules (Fig. 8D) and gypsum rosettes (Fig. 8C) mark them as Aridisols (Soil Survey Staff, 1999) and Calcic Gleysols (Food and Agriculture Organization, 1974). Weakly developed paleosols (Barathi, Budi, Pawa) are of less consequence to the stable soilscape of the earliest Triassic dominated by Calcic Xerosols. This is most like modern soils of the loessic piedmont of Tashkent, Fergana, and Samarkand, Uzbekistan (map unit Xk 4–2ab of Food and Agriculture Organization, 1978a). Tashkent is semi-arid, cool, and continental. Mean annual precipitation is 417 mm (141–643 mm), and mean annual temperature is 13.5 °C (6.7–18.9 °C), with July hotter (27.4 °C) and drier (12 mm) than

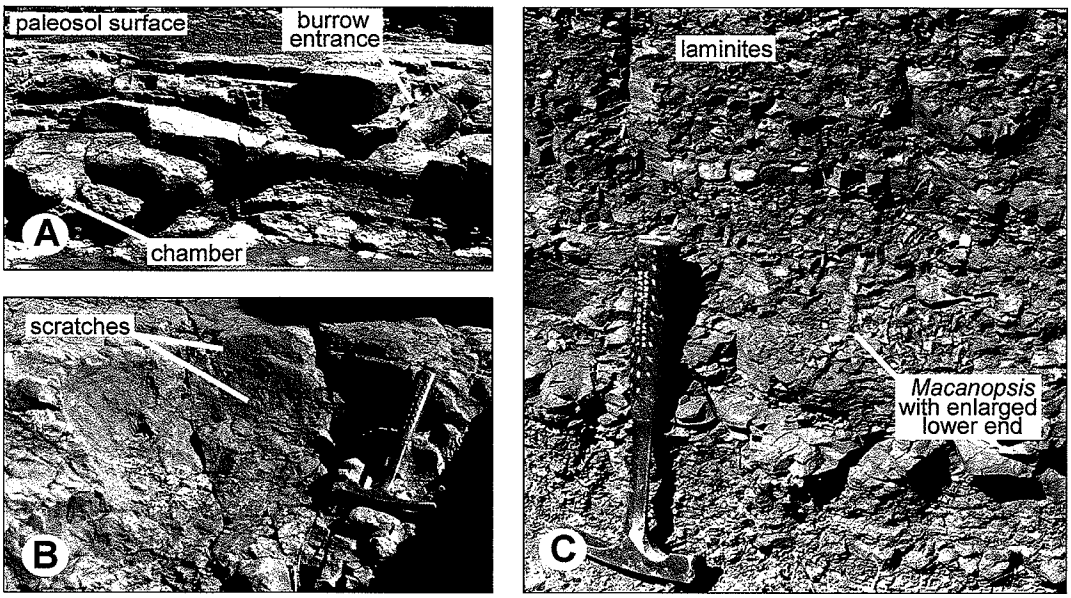

Figure 10. Burrow like those containing skeletons of *Lystrosaurus* in Patha paleosol near Bethulie (A), open burrow or wallow in a Som paleosol near Lootsberg pass (B), and likely crustacean trace fossil *Macanopsis* from Zam paleosol at Lootsberg Pass (C). Hammers are for scale. Flaring toward terminal turnaround can be seen toward base of *Macanopsis*. Entrance to *Lystrosaurus* burrow faces into outcrop, then curves around to living chamber jutting out of outcrop in an incomplete helicoidal form.

January (-1.1 °C, 49 mm: Müller, 1982). Vegetation is Turanian wooded grassland with scattered trees and shrubs of juniper (*Juniperus polycarpos*), pistacia (*Pistacia vera*), and almond (*Amygdalus bucharica*: Zohary, 1973). Open woodlands and wooded grasslands also grow in such sodic soils in Southern Africa, where the dominant tree is mopane (*Colophospermum mopane*: Food and Agriculture Organization, 1977) and in Australia, where the dominant trees are mallee (*Eucalyptus oleosa*) and Murray pine (*Callitris preissii*: Stace et al., 1968; Food and Agriculture Organization, 1978b).

SOIL AND SEDIMENTARY ENVIRONMENTS

Even apart from their classification, various features of paleosols reveal specific aspects of ancient environments (Table 2). Some factors in soil formation inferred from paleosols, such as time for formation, paleotopography, and parent material, augment and support evidence from published accounts of the alluvial sedimentary environments of the Permian–Triassic boundary in the Karoo Basin (Smith, 1990, 1993a, 1993b, 1995).

Parent material for the paleosols is the sediment itself, which is derived in large part from erosion of the Paleozoic Cape Fold belt, to the south (Hiller and Stavrakis, 1984; Veevers et al., 1994; Haycock et al., 1997; Catuneanu and Elango, 2001). This sandy and silty alluvium was largely quartz and feldspar, but metamorphic rock fragments are also common. A few elongate grains, now quartz, may have originally been volcanic glass shards. Rare grains of biotite indicate a minor volcanic component. None of these volcanic grains is glassy or fresh, and they may have been eroded from earlier Permian tuffs of the Ecca Group to the south (Johnson, 1991; Veevers et al., 1994). The high depositional energy of near-stream environments, as inferred from trough cross-bedded sandstones, and linguoid rippled siltstones (Smith, 1995), is reflected in sandy quartzose alluvium, which formed a relatively nutrient-poor (oligotrophic) parent material to some of the paleosols (Hom, Du, and Budi pedotypes of Table 2). Other pedotypes formed on clayey and more fertile (higher Na, K, Ca, Mg) floodplains; they were redeposited from soils and sediments formed elsewhere in the depositional basin and eroded from Paleozoic shales. A surprising outcome of point-counting was the discovery of high amounts of angular silt (Figs. 5, 6, and 11). In thin section, Karoo paleosols are very similar to paleosols of loess such as the Quaternary Palouse Loess of Washington, USA, which are derived largely from wind redeposition of glacial outwash and volcanic ash (Busacca, 1989). Both latest Permian and earliest Triassic landscapes were dusty and dry, with much sediment transported by dust storm winds as well as by seasonal flash floods. The Cape Fold Belt and contiguous Gondwanan mountain ranges of South America and Antarctica were volcanically active and probably also glaciated at such high paleolatitude (Veevers et al., 1994).

Paleotopographic position of paleosols within sedimentary environments is revealed by features of paleosols reflecting former water tables. Some paleosols (Karie, Kuta, and Patha) have prominent large burrows (Fig. 10A) and other open excavations comparable to those made by animals grubbing for water or tubers (Fig. 10B). Some of the burrows contain articulated skeletons of the air-breathing animals *Lystrosaurus*, *Thrinaxodon*, and *Procolophon* (Groenewald, 1991; Smith, 1995), which would not have excavated below water table. Also seen in Karie paleosols were scratched and lined burrows with meniscate backfill (left hand side Fig. 8B; trace fossil genus *Scoyenia*; see Häntzschel, 1975) that are comparable to burrows of soil bugs and millipedes (Retallack, 2001a). Fossil millipedes comparable to living *Gymnostreptus* have been found in the *Lystrosaurus* zone at Bethulie (Rubidge, 1995; MacRae, 1999; Lawrence, 1984). *Scoyenia* burrows and clay skins seen in thin sections (Fig. 8B) extend down to the depth of reddening and low ratios of FeO/Fe_2O_3 in these paleosols, so that the oxidation, if not the final diagenetically altered red hue (Retallack, 1991a), is an indication of good

TABLE 2. INTERPRETATION OF PEDOTYPES ACROSS PERMIAN–TRIASSIC BOUNDARY

Pedotype	Paleoclimate	Former vegetation	Former animals and trace fossils	Paleotopography	Parent material	Time for formation
Triassic paleosols (*Lystrosaurus* zone)						
Barathi	Unknown	Early successional quillwort marsh	*Skolithos, Lystrosaurus*	Lake, anabranch margin	Quartzofeldspathic silty clay	0.1 (0.1–0.5) ka
Budi	Unknown	Early successional horsetail marsh	*Macanopsis*	Riverside swale	Quartzose sand	0.1 (0.1–0.5) ka
Karie	Subhumid seasonal	Dry woodland	*Scoyenia, Histioderma, Lystrosaurus*	Dry floodplain	Quartzofeldspathic silty clay	6 (5–8) ka
Kuta	Subhumid moderately seasonal	Dry woodland	*Histioderma, Lystrosaurus*	Dry floodplain	Quartzofeldspathic silty clay	6 (5–8) ka
Patha	Unknown	Riparian bushland	*Macanopsis, Scoyenia, Histioderma, Owenetta,* Whaitsiid, *Proterosuchus, Lystrosaurus*	Streamside levee	Quartzofeldspathic silty clay	1.5 (1–2) ka
Sedibo	Subhumid, seasonally wet	Riparian woodland	*Macanopsis*	Lake margin	Quartzofeldspathic silty clay	6 (5–8) ka
Permian paleosols (*Dicynodon* zone)						
Bada	Semi-arid, long dry season	Seasonally wet, dry bushland	*Dicynodon, Lystrosaurus*	Floodplain depression	Quartzofeldspathic silty clay	10 (8–15) ka
Du	Unknown	Early successional bushland	None found	Streamside sand bar	Quartzose sand	0.1 (0.1–0.5) ka
Hom	Unknown	Seasonally wet, riparian bushland	*Lystrosaurus*	Streamside sandy levee	Quartzose sand	6 (5–8) ka
Pawa	Unknown	Early successional horsetail marsh	*Skolithos, Macanopsis*	Streamside clayey swale	Quartzofeldspathic silty clay	0.1 (0.1–0.5) ka
Som	Semi-arid, long dry season	Seasonally wet bushland	*Lystrosaurus, Moscorhinus*	Dry floodplain	Quartzofeldspathic silty clay	3 (2–5) ka
Zam	Unknown	Early successional quillwort marsh	*Macanopsis, Lystrosaurus*	Lake margin	Quartzofeldspathic silty clay	0.1 (0.1–0.5) ka

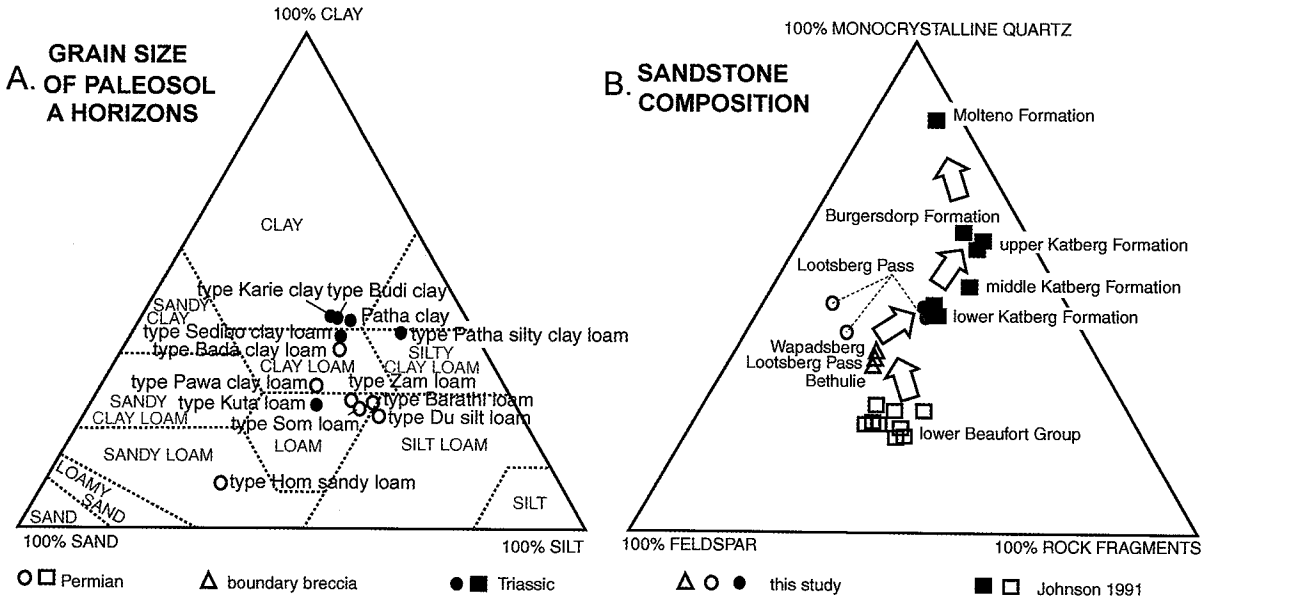

Figure 11. Point-counted sand-silt-clay composition of paleosols (A) and quartz-feldspar-lithic composition of sandstones (B) in Permian–Triassic boundary beds, compared with results for older and younger Karoo rocks from Johnson (1991).

drainage. Other paleosols (Budi, Sedibo, Pawa) in contrast, contain oblique, silt-filled, irregularly scratched burrows with terminal chambers (Fig. 10C; trace fossil genus *Macanopsis*; see Häntzschel, 1975). *Macanopsis* is widely assumed to have been made by crustaceans, which may have lived in submerged burrows, but spiders and beetles also make comparable burrows (Ratcliffe and Fagerstrom, 1980). Nevertheless, some paleosols with *Macanopsis* burrows lack red hue or clay skins and have hollow isoetalean root traces (Fig. 9A) and so may have been poorly drained. Deep root traces and calcareous nodules in some of these paleosols (Bada, Hom, Sedibo) indicate that the water table dropped quite low within the profile for a part of the year, but other paleosols (Budi, Pawa) may have been more permanently waterlogged at depth. Many of these gray paleosols (Hom, Du, Pawa, Sedibo) are immediately below or within sandstone paleochannels, as if they were formed within anabranches of braided streams, chutes of levees, crevasse-splay chan-

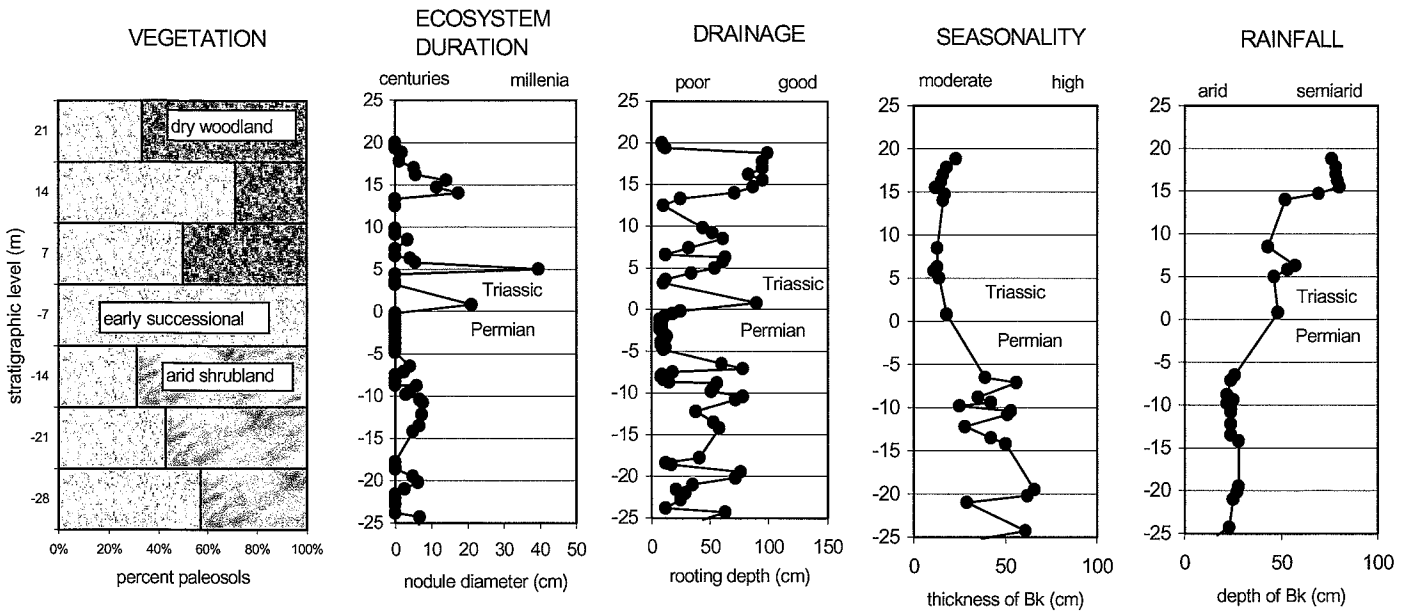

Figure 12. Changes in proxy measures of vegetation, ecosystem duration, soil drainage, seasonality, and rainfall across Permian–Triassic boundary at Lootsberg Pass. Zero level is Permian–Triassic boundary breccia datum of Figure 4.

nels, or other near-stream swales. This is not true of Bada paleosols, which represent a widespread floodplain environment in which the water table dropped at least a meter below the surface to allow root and nodule growth. Root trace lengths were measured in paleosols of the Lootsberg Pass section as a guide to water-table depth, because roots respire and must be moderately aerated for most of the year. The best drained earliest Triassic paleosols were better drained than the best drained latest Permian paleosols (Fig. 12), and this change in base level may anticipate progradation of sandy alluvial fans of the Katberg Formation (Hiller and Stavrakis, 1984; Smith, 1995). Nevertheless, this change in drainage is modest, and there were local poorly drained paleosols in both Permian and Triassic, especially within the laminate facies at the Permian–Triassic boundary.

The impression that the Karoo sequence is a high-resolution record of latest Permian and earliest Triassic time (Smith and Ward, 2001) is confirmed by a generally weak to moderate degree of paleosol development. Estimated times for formation of the paleosols can be assigned by comparing their nodule sizes. Five nodule diameters were measured and averaged from each paleosol with nodules in the Lootsberg Pass section as a proxy for changing soil and ecosystem durations. The biggest nodules in this section are just below the boundary, but paleosols in overlying earliest Triassic rocks are poorly developed, whereas paleosols in underlying latest Permian rocks are generally better developed (Fig. 12).

TABLE 3. RATES OF ACCUMULATION (MM/YR) ESTIMATED FROM PALEOSOLS

Facies	Lootsberg Pass	Carlton Heights	Bethulie
Triassic floodplain	0.26	0.25	0.36
boundary laminites	1.10	0.34	1.62
Permian floodplain	0.15	0.14	0.16

Another approach is to estimate time for formation of paleosols from nodule abundance and clay content by comparison with well-dated Quaternary soils near Las Cruces, New Mexico (Gile et al., 1980). Bada paleosols are comparable in these respects to Isaaks Ranch soils dated at 8–15 ka, and Som paleosols are similar to Organ soils dated at 2–5 ka. Sedibo, Kuta, and Karie paleosols fall between these in their degree of development. At the other extreme are very weakly developed paleosols with abundant relict bedding and thickness less than 10 cm, which are unlikely to represent more than 100 yr of plant growth in arid climates. Applying these order of magnitude time estimates (Table 2) to the distribution of paleosols in each measured section (Fig. 4) gives a consistent history of sedimentation at each section (Table 3), which was slow during the Permian, accelerated greatly during the terminal Permian laminites, and remained high during the earliest Triassic. All of these estimates are within clayey facies of the upper Palingkloof Member of the Balfour Formation. Each site was overrun by thick, laterally extensive paleochannel sandstones of the Katberg Formation, interpreted as a marked shift toward braided stream morphology and higher sedimentation rates by Ward et al. (2000). This pattern of accelerating rates of sediment accumulation into the Permian–Triassic boundary is also seen in paleosol sequences of Australia (Retallack, 1999a) and Antarctica (Retallack and Krull, 1999). This pattern may reflect uplift of the entire Gondwana-margin mountain range (Veevers et al., 1994; Groenewald and Rust, 1998). It could also reflect climatic change to greater humidity and growth of montane ice caps, with increased earliest Triassic erosional scouring and uplift by isostatic compensation (following general arguments of Molnar and England, 1990).

PALEOCLIMATIC CHANGE

Calcareous nodules in soils are climatically sensitive in two ways. First, the spread of carbonate nodules through a profile is related to climatic seasonality, with nodules scattered throughout the profile in monsoonal climates like that of Pakistan (Sehgal et al., 1968; Retallack, 1991b), but more focused within the

profile in less seasonal climates like that of New Mexico (Gile et al., 1980). Second, the depth to calcareous nodules is related to mean annual precipitation, so that nodules are shallower in drier climates (Retallack, 1997a). These indications of paleoclimate could be compromised by surficial erosion or eolian addition to the paleosols. Significant erosion is unlikely in a sequence of such high sediment accumulation rate (Table 3), where claystone breccia is rare, paleosols have such well-preserved root traces (Fig. 9B) and burrows contain articulated unweathered skeletons (Fig. 10A; Smith, 1995). Eolian overthickening of paleosols would give smaller nodules in paleosols with deeper calcic horizons, but no such relationship was observed (Fig. 12). All three Permian–Triassic sections examined show shallower, less focused nodules in the Permian than the Triassic, indicating a strongly seasonal, arid, Permian paleoclimate, but a less seasonal, semiarid to subhumid Triassic paleoclimate (Figs. 4 and 7).

Seasonality, probably with winter snow, is indicated by banded clay-skins (Fig. 8B) and varve-like shale fragments in both Permian and Triassic paleosols (Fig. 8A). Seasonality is also indicated by Permian and Triassic fossil trees with pronounced growth rings near Harrismith and Senekal (Warren, 1912; Walton, 1925; du Toit, 1939; Plumstead, 1969; Haughton, 1970; Hancox et al., 2002). Such cool, seasonal paleoclimate is compatible with high Permian–Triassic paleolatitudes of the Karoo Basin (Veevers et al., 1994).

A wetter Triassic than Permian paleoclimate is consistent with increasingly quartz-rich sandstone compositions through time (Fig. 11B), although this also could be due to greater exhumation of Paleozoic quartzites of the Cape Fold Belt from beneath earlier Permian sedimentary cover (Veevers et al., 1994). Feldspar and rock fragments are more readily weathered than quartz, and as chemical weathering increases in humid climates, the proportion of quartz in sediments increases (Suttner and Dutta, 1986). More humid weathering may also explain why Triassic paleosols and sediments are richer in alumina than Permian ones (Fig. 5), an effect also noted along with greater Triassic depletion of rare earth elements in the Permian–Triassic sequence near Senekal (Hancox et al., 2002). A wetter Triassic than Permian paleoclimate also is indicated by increased abundance of lycopsid spores and roots (Stapleton, 1978; Steiner et al., 2001), larger size of fossil leaves (Anderson and Anderson, 1985) and logs (Warren, 1912; Walton, 1925; du Toit, 1939; Plumstead, 1969; Hancox et al., 2002), and greater abundance and diversity of labyrinthodont amphibians (Parrington, 1948; Rubidge, 1995). The transition to braided from meandering streams across the Permian–Triassic boundary is not necessarily evidence of drier climate. Vegetation may have been thinned by plant extinction for other reasons, or rainstorms may have become more violent than could be withstood by vegetation (Ward et al., 2000). Nor does the shift to redder Triassic than Permian paleosols necessarily indicate a drier climate (Hiller and Stavrakis, 1984; Smith, 1995), because it reflects instead good soil drainage and deep root penetration with alluvial fan progradation (Fig. 12). Although red color has often been regarded as evidence of desert climates, deserts are red when their bedrock is red (as in Kyzl Kum desert), and gray when bedrock is gray (as in neighboring Kara Kum desert), because there is insufficient moisture for iron release and oxidation of bedrock. The red bedrock of modern deserts is often a sequence of humid-climate paleosols of Miocene or older age (Retallack, 1997a). There are many deeply weathered red soils and Triassic paleosols of humid paleoclimates (Retallack, 1999a; Retallack and Krull, 1999), as well as red soils and Triassic paleosols of arid paleoclimates (Mader, 1990).

Quantitative estimates of mean annual precipitation (P in mm) can be obtained from the depth to calcareous nodules (D in cm) by using the following transfer function:

$$P = 139.6 + 6.388D - 0.01303D^2,$$

with standard deviation ± 141 mm and correlation coefficient of 0.8 (Retallack, 1997a; 2000; Royer, 1999). For application to paleosols, measured depth was corrected for compaction (Sheldon and Retallack, 2001). Corrections were not made for differences in atmospheric CO_2 compared with modern ($10^{-3.5}$%) assumed for the transfer function. Levels of CO_2 were high during the latest Permian ($10^{-2.8}$%) and abruptly higher during the earliest Triassic ($10^{-2.5}$%), judging from stomatal index data (Retallack, 2001b, 2002a). A numerical model of pedogenic carbonate depths by McFadden and Tinsley (1985) reveals that the effect of such high CO_2 is small in comparison with soil respiration effects. Their model can be used to calculate that the CO_2-effect would give Permian paleoprecipitation estimates 20 mm lower and Triassic estimates 40 mm lower than assuming a modern atmosphere, which are small considering error bars and calculated magnitude of the change. Our uncorrected paleoprecipitation estimates can be put on a time scale using an approximate age model derived from comparisons with Quaternary soils (Tables 2 and 3) to calculate changes in mean annual precipitation through time in each of the measured sections. From these calculations for Lootsberg Pass, latest Permian precipitation is interpreted to have been 346 ± 141 mm (average of 15 estimates), whereas earliest Triassic precipitation is interpreted as 732 ± 141 mm (average of 12). Paleosols at Carlton Heights and Bethulie show similar values and trends (Fig. 13).

These observations can be placed within a regional context by similar calculations for Permian and Triassic calcareous paleosols observed in other parts of South Africa. Four latest Permian paleosols in the Steenskampsvlatke Member above Teekloof Pass (Rubidge, 1995) had calcareous nodules at depths of 15, 15, 16 and 18 cm, respectively. In contrast, three earliest Triassic paleosols near Harrismith had calcareous nodules at 80, 88, and 90 cm, and two paleosols at the same stratigraphic level near Bergville had nodules at 92- and 95-cm depth within the profile (Retallack, 1997a, color photo 88). These data, added to those from the sections measured (Fig. 4), show a clear trend of wetter climate toward the east (Fig. 13), with earliest Triassic wetter than latest Permian at any given locality. Latest Permian rocks in Natal include pedogenic carbonate nodules not yet measured (Botha and Linström, 1978), but no Triassic rocks are exposed at Teekloof Pass (Rubidge, 1995). The observed trend (Fig. 13) predicts that late Permian paleoprecipitation in Natal was similar to early Triassic at Teekloof Pass. Because of the persistence of similar climate in other areas, regional mass extinctions are unlikely to be due to these modest changes in precipitation, temperature, or water table. The paleoclimatic gradient is less steep than the current precipitation gradient in the same region (Fig. 13). The steeper modern gradient is due, in part, to higher elevation to the east, whereas the Permian–Triassic depositional basin would have had low relief (Veevers et al., 1994; Smith, 1995). Maintenance of the same climatic gradient with precipitation wetter in the Triassic than Permian is evidence for regional climate change rather than a local effect of an advancing alluvial fan or rain shadow.

Yet other paleoclimatic proxies can be gained from the chemical composition of paleosol-B horizons by comparison with modern soils (Sheldon et al., 2002):

$$P = -259.34 \ln B + 759.05,$$

$$T = -18.516S + 17.298,$$

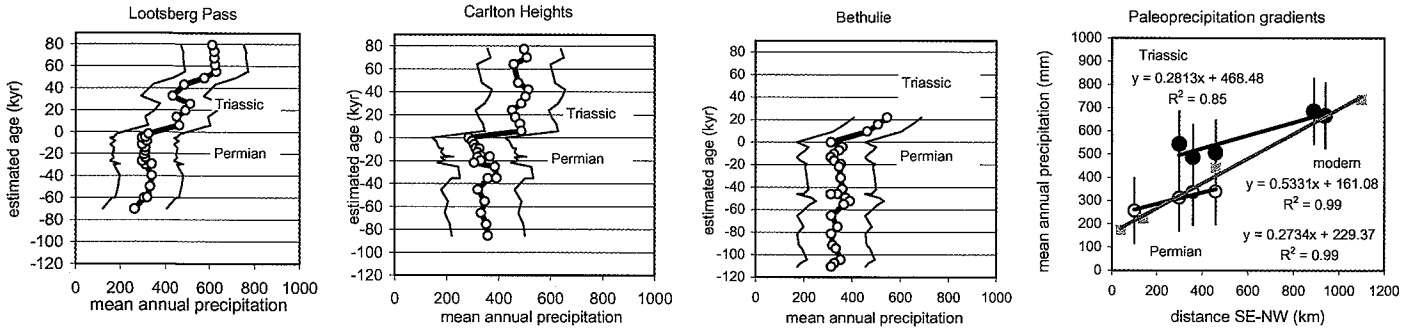

Figure 13. Mean annual paleoprecipitation for Lootsberg Pass, Carlton Heights, and Bethulie sections, estimated from depth to calcic horizon and on a time scale estimated from degree of development of paleosols (Table 2). Zero level is Permian–Triassic boundary breccia datum of Figure 4. To right is average mean annual precipitation for these and additional soils and paleosols on a 1200-km transect from Cape Province to Natal. Triassic paleosols were wetter than Permian paleosols at each site, and both showed lower paleoprecipitation gradients but precipitation comparable to the same region today.

where P is mean annual precipitation (± 235 mm, R^2 = 0.7), T is mean annual temperature in °C (± 4.4 °C, R^2 = 0.4), B is molecular ratio of bases/alumina, and S is molecular ratio of potash and soda to alumina. Only three paleosols at Lootsberg Pass were analyzed: latest Permian Bada paleosol with a temperature of 9.9 °C and precipitation of 740 mm, the earliest Triassic Kuta paleosol with 10.3 °C and 801 mm, and early Triassic Karie paleosol with 10.3 °C and 783 mm. These results indicate a more humid and warmer Triassic than Permian, as do geochemical results of Hancox et al. (2002) in the northern Karoo Basin. The resolution of these calculations is disappointing, perhaps because paleosol chemical composition has been compromised by diagenetic mass transfer of alkali and alkaline earth elements (de Wit et al., 2002). Nevertheless, cold and dry conditions for both Permian and Triassic are confirmed.

Increased temperature also can be inferred across the Permian–Triassic boundary from a negative oxygen isotopic shift ($\delta^{18}O$) in therapsid tusks and pedogenic carbonate nodules at Lootsberg Pass and Bethulie (Smith and MacLeod, 1998; MacLeod et al., 2000). Comparable isotopic shifts in marine carbonates have also been used to argue for a temperature increase of as much as 6 °C across the Permian–Triassic boundary in the tropics (Holser et al., 1991), but estimation of the warming's magnitude is compromised by burial diagenetic alteration of marine carbonate (Mii et al., 1997). Burial diagenesis also is likely to have affected Karoo carbonate nodules, and perhaps also the tusks (de Wit et al., 2002). Paleosols interpreted as Ultisols in Antarctica are evidence of warm, temperate early Triassic conditions within the polar circle, because these sites were at a paleolatitude of 65–77 °S, yet such soils do not develop now at latitudes any higher than 48° (Food and Agriculture Organization, 1978a, 1978b; Retallack and Krull, 1999). Warmer and wetter paleoclimate over much of the Gondwana supercontinent confirms an earliest Triassic postapocalyptic greenhouse (Retallack, 1999a).

PLANT EXTINCTION

Only very fragmentary plant remains and root traces, lacking original carbon, were found along with latest Permian and earliest Triassic paleosols. These fossils, as well as the very different profile forms of the paleosols, indicate pronounced plant extinction at the Permian–Triassic boundary in support of paleobotanical records elsewhere (Retallack, 1995; Looy et al., 2001).

Most latest Permian root traces in Bada, Som, Du, and Hom paleosols are narrow, copiously branched, and have a striated surface texture characteristic of woody plants (Fig. 9B), which at this point in Earth history would have been gymnosperms or progymnosperms rather than angiosperms. Although these may have been tree roots, low desert shrubs can also have substantial woody root systems. A paleochannel lag (at −18 m) in the Lootsberg section contained flattened impressions of logs up to 12.8 cm across. This is the original diameter, according to Walton's (1936) compaction hypothesis, and would have been a tree at least 8 m high using Whittaker and Woodwell's (1968) regressions for modern pine (*Pinus rigida*). Thus, riparian vegetation included small trees. Also found in Pawa paleosols were fine root traces with abundant orthogonal laterals, comparable with fossil equisetalean adventitious roots (see Mader, 1990). In Zam paleosols, short, sparsely branched, hollow roots (Fig. 9A) are comparable with those of quillworts (*Isoetes*) and other lycopsids (Retallack 1997b). Living quillworts thrive both under water and in wet meadows, and both options are likely for Zam (oxidized) and Pawa (unoxidized) paleosols in the laminites (Figs. 3 and 4).

Latest Permian paleosols of the central Karoo Basin are equivalent in age to the Estcourt Formation, a sequence of coal measures formed in more humid paleoclimate to the northeast in Natal, for example, near Bulwer. The flora of the Estcourt Formation includes a variety of *Glossopteris* leaves, which are small (typically 8–12 cm long) and narrow-meshed for this genus, associated with a distinctive set of reproductive structures (*Lidgettonia*, *Rigbya*) and with gleyed paleosols riddled with carbonized glossopterid roots *Vertebraria* (Anderson and Anderson, 1985). The conspicuous absence of *Vertebraria* in paleosols from Bethulie to Lootsberg indicates that vegetation in dry soils to the west was very different. The gymnosperm component may have included conifers or glossopterids, which would have been small-leaved in such a dry climate. The Australian latest Permian glossopterid *Blechnoxylon talbragarense* had small (1.2-cm-long), thick (0.2 mm), recurved pilose leaves, arranged in short shoots with scale-like bracts, and stout (3-mm in diameter), divaricating spinose stems with secondary wood and short internodes (Etheridge, 1899, White, 1986). This kind of growth habit is common today in overgrazed shrubs of arid lands, such as small-leaved African species of *Boswellia*, *Commiphora*, and *Rhus*. Also found in inland parts of the Australian latest Permian is the supposed conifer *Walkomiella* (White, 1986), known from the Ecca Coal Measures of South Africa (Anderson and An-

derson, 1985). Unlike Permian and modern conifers with comparable scale-like leaves, *Walkomiella* has branches at low angles that are sometimes dichotomizing rather than rectilinear and monopodial, and its cones are terminal and coaxial with long shoots rather than bent to one side of short shoots. Although it has been compared with monkey-puzzle trees (*Araucaria*), *Walkomiella* could well have been a desert shrub, comparable with modern karooid shrubs such as *Pentzia*. Other gymnosperms notable for their small leaves are *Pagiophyllum vandijkii* and *Benlightfootia mooiensis* from the Estcourt Formation of Natal (Anderson and Anderson, 1985). Equisetalean and lycopsid roots are mostly in riparian or lacustrine sediments, but some may also have been desert ephemerals (Mader, 1990).

Earliest Triassic paleosols include a comparable array of woody gymnosperm roots (in Kuta, Karie, and Sedibo paleosols); fine, orthogonally branched roots of equisetaleans (in Barathi paleosols); and sparsely branched, hollow roots of lycopsids (in Budi paleosols). Greater depth to carbonate and indications of greater desalinization of these paleosols are evidence for more mesic vegetation than during the late Permian. The boundary laminites (Figs. 3 and 4) have only small, hollow root traces like those of herbaceous quillworts (Fig. 9A), but this phase of herbaceous vegetation was short lived (Fig. 12) and soon supplanted by woody vegetation in Kuta and other paleosols. Looy (2000) and Looy et al. (2001) have argued that earliest Triassic vegetation was dominantly herbaceous, but pollen of woody gymnosperms remains common even in earliest Triassic samples, and woody root traces are common in earliest Triassic paleosols in South Africa and elsewhere (Retallack, 1999a; Retallack and Krull, 1999).

Permineralized fossil logs of conifers, including one of *Dadoxylon sclerosum* 29-m long, are known from the Katberg Formation near Harrismith (Warren, 1912; Walton, 1925; du Toit, 1939; Plumstead, 1969; Haughton, 1970) and from the Vervkykerskop Formation near Senekal (Hancox et al., 2002). Fossil plants of the *Lystrosaurus* zone reported by Rubidge (1995) are not Triassic because of biostratigraphic revisions (Smith and Ward, 2001), but from the latest Permian at Kilburn Dam, Natal (Anderson and Anderson, 1985). During our study, fossil plant hash was found at two localities in the basal Katberg Formation: in the highway cut at 18 m in the Carlton Heights section and in a spur northeast of the waterfall at 15 m in the Bethulie section (Fig. 3). This fossil flora included small (3-mm) ovoid seeds, fragments of lycopsid corms, fragments of seed fern leaves, and small (5 × 2 mm) conifer needles. This fragmentary flora is similar to one dominated by the seed fern *Lepidopteris callipteroides*, the conifer *Voltziopsis africana*, and the quillwort *Isoetes beestoni* from bed 4 of the Sakamena Group in Madagascar, and from the basal Narrabeen Group in the Sydney Basin, southeastern Australia (Retallack, 1997b, 2002b). Open woodland envisaged for the earliest Triassic of the Karoo Basin contrasted with riparian gallery woodland and arid shrubland envisaged for the latest Permian.

VERTEBRATE EXTINCTION

Our collections from South Africa indicate a pronounced and geologically abrupt extinction of vertebrates at the Permian–Triassic boundary, with a diversity minimum in the poorly fossiliferous laminites (Smith and Ward, 2001). This may be, in part, a taphonomic artefact, and the extinctions even more abrupt because weakly developed paleosols like those of the laminites commonly have fewer fossil bones than alkaline, moderately developed soils in which bone accumulated (Retallack, 1998). Above the laminites, this taphonomic artifact is less likely because the upper Palingkloof Member and Katberg Sandstone are richly fossiliferous and their paleosols are well developed and strongly calcareous (Smith, 1995). The latest Permian uppermost *Dicynodon* zone has 34 genera of terrestrial vertebrates, but the earliest Triassic *Lystrosaurus* zone has only 17 mainly different genera, for an extinction of 88% of genera (Rubidge, 1995).

The ecology of *Lystrosaurus*, as constrained by its context in paleosols, is of interest in understanding the nature of this extinction. *Lystrosaurus* was a survivor from the Permian rather than a newly evolved Triassic genus, but it is more abundant after the boundary than before. It is found in virtually all of the Triassic pedotypes, and in many Permian pedotypes (Table 2); thus, it lived in a wide range of habitats. The coexisting dicynodont of the latest Permian, *Dicynodon*, is also represented by numerous specimens, but mainly from Bada paleosols, indicating preference for arid shrubland habitat. Environmental flexibility may have been an advantage for survival in this life crisis.

Burrowing may also have aided survival, and is documented for Karoo Basin Permian and Triassic cotylosaurs (*Procolophon*) and therapsids (*Lystrosaurus*, *Diictodon*, *Trirachodon*: Smith, 1987; Groenwald et al., 2001). These extinct animals had a bone structure and body shape comparable to those of modern burrowing rodents (King, 1993). Within the sites selected for this study (Fig. 4), three articulated skeletons of *Lystrosaurus* were found in large scratched burrows, which have been assigned to the ichnogenus *Histioderma* by Groenewald (1991). The burrows differ from *Histioderma* (see Häntzschel, 1975) in their large size (20–30 cm in diameter, 2–3 m long, turnarounds 1 m long at depths of up to 48 cm) and by curving in an horizontal plane in the form of a helix that does not complete a rotation (Fig. 10). All three observed earliest Triassic skeletons in the burrows were small (basal skull length 11–12 cm) and had curved skulls (as in *Lystrosaurus curvatus* and *L. declivis* of Cluver 1971). These burrows with *Lystrosaurus* were only seen in the earliest Triassic part of the sequence, not in laminites or lower rocks. In the type Kuta paleosol, for example, there is a large burrow filled with sand from the overlying sandstone paleochannel, as well as a very sandy surface to the profile penetrated by root traces below the paleochannel. This sandy surface is probably material excavated from the sandy subsurface of the soil. On the Russian steppe today, the Bobak marmot (*Marmota bobac*) is a comparably large animal; it makes burrows surrounded by mounds of excavated earth 25–30 m in diameter and 0.3–1.5 m high (Lavrenko and Karamysheva, 1993). These burrows contribute to desalinization and decalcification of the soil and engender a patchy distribution of vegetation. Such an effect may explain the more pronounced subsurface salinization and calcification of the Kuta paleosol, which was sampled near a burrow, than the Karie and Bada paleosols, which were unburrowed where sampled (Fig. 5). Furthermore, root traces in the Kuta paleosol were clay filled and non-calcareous, whereas calcareous rhizoconcretions were found in both Karie and Bada paleosols. Mound and intermound vegetation probably differed, forming a patchy mosaic of eutrophic plants of alkaline soil and oligotrophic plants of acidic soil. Burrows and small size may have offered advantages for both animal and plant survival of the Permian–Triassic life crisis.

The idea that *Lystrosaurus* was aquatic (Cluver, 1971) is no longer thought likely, considering its short tail, stubby limbs, and fingers (King and Cluver, 1991), and the well-drained paleosols in which it walked and burrowed, as outlined here and elsewhere (Retallack, 1996; Retallack and Hammer, 1998). Nevertheless, *Lystrosaurus* also occurred with weakly developed paleosols (Zam pedotype), which supported emergent and submerged

quillworts (*Isoetes*), probably a preferred fodder of therapsid herbivores (Retallack, 1997b) compared with less nutritious and highly siliceous horsetails (*Phyllotheca*, *Neocalamites*; Rayner, 1992). *Lystrosaurus* may have waded into water for food but had wider environmental tolerances. There was more water and less saline water at the beginning of the Triassic, as indicated by the paleosols reported here, and a dramatic evolutionary radiation of labyrinthodonts (Parrington, 1948; Rubidge, 1995).

The flat face, large snout, and elevated nostrils and eye sockets of *Lystrosaurus*, originally cited as evidence of aquatic habits, are similar to those of the Oligocene oreodont *Leptauchenia*, which also has been regarded as amphibious and is also found in dusty aridland paleosols (Retallack, 1983). Comparable amphibious interpretations have been made for the elevated nares of Jurassic sauropods, which also lived in dry dusty environments (Retallack, 1997c). Also comparable are the elevated eyes and long nose of the saiga antelope (*Saiga tatarica*), which Knystautus (1987) argues is an adaptation mitigating dust inhalation in a dry, dusty landscape. Both Permian and Triassic paleosols with *Lystrosaurus* have abundant angular silt grains (Figs. 5, 6, and 11) like those of loess.

Other adaptive features of *Lystrosaurus* tally with cold paleoclimate reconstructed from paleosols. The compact dicynodont form, with short tail, stout legs, and short neck, could be an example of Allen's Rule, whereby animals of cold climates have reduced extremities for heat conservation (Brown and Lomolino, 1998). Bergmann's Rule is another such rule of thumb that animals become larger with latitude, again for heat conservation (Brown and Lomolino, 1998). A cold latest Permian, followed by slightly warmer earliest Triassic, as revealed by paleosols, is accompanied by decreasing size of dicynodonts in accordance with these ideas.

Yet other features of *Lystrosaurus* are respiratory adaptations. The internal nares of *Lystrosaurus* and subsequent Triassic dicynodonts are less than 60% of the length of the interpterygoid space, whereas in *Dicynodon* and other Permian therapsids the internal nares are more than 60% as long as the interpterygoid space (Cruikshank, 1968; Maisch, 2002). This was a critical threshold in the evolution of separate buccal and nasal cavities (King, 1991) and would have been adaptive in both hypercapnic (excess CO_2) or hypoxic (low O_2) conditions. A second peculiarity of *Lystrosaurus* is its expanded chest, thick ribs, and elongated neural spines, especially compared with the weasel-like form of *Dicynodon* and *Diictodon* (Fig. 2). Such a large chest also is apparent in a very complete skeleton of an archosaur (*Proterosuchus vanhoepeni*) from the earliest Triassic (Haughton, 1970). Associated cynodont carnivores are highly cursorial in both Permian and Triassic, but Triassic *Galesaurus* and *Thrinaxodon* have expanded upper ribs and long vertebral spines. Some of this expanded visceral cavity and back could have been for an enlarged stomach for digesting large quantities of low-quality food (Hotton et al., 1997), as suggested by the indiscriminate habitat preferences of *Lystrosaurus* compared with *Dicynodon*, as inferred from paleosol occurrences (herein; Retallack and Hammer, 1998), but this does not account for the reduced size of lumbar ribs in carnivores. Another explanation for thickened thoracic ribs, higher thoracic vertebral spines, and reduced lumbar ribs, is enlarged lungs and a mammal-like, muscular diaphragm (Brink, 1956; King, 1991). There also has been speculation (by Graham et al., 1997) that Late Permian hypoxia selected for evolution of continuous, rhythmic respiration, of endothermy, and of separate systemic and pulmonary circulation in a four-chambered heart, which distinguish mammals from reptiles. These various increases in ventilation and circulatory capacity also would have been advantageous under conditions of hypercapnia and dustiness. Along with hypoxia, these are all hazards of burrowing, for which there is trace fossil evidence in both Permian and Triassic rocks (Smith, 1987, 1993b; Groenewald, 1991; Groenewald et al., 2001). A postapocalyptic greenhouse inferred here from paleosol evidence for an increase in humidity and warmth from Permian to Triassic could have been severe enough to dilute atmospheric oxygen content with greenhouse gases such as carbon dioxide, methane, and water vapor (Krull et al., 2000; Berner, 2002). Respiratory adaptations to burrowing could have been critical for survival in a global atmospheric crisis.

MECHANISMS OF EXTINCTION

A variety of extinction mechanisms have been suggested for the Permian–Triassic life crisis, and each can be tested against the new evidence of environmental change presented here (Figs. 14 and 15). Extinction by asteroid or comet impact, for example, can be envisaged as a preplay of a widely accepted scenario for the terminal Cretaceous extinction of dinosaurs (Becker et al., 2001). Boundary beds in the northern Karoo Basin have no more than 320 ppt iridium (Hancox et al., 2002), which is the same order of magnitude as iridium in boundary beds of Antarctica, Australia (Retallack et al., 1998), and China (Zhou and Chai, 1991), and well short of iridium abundance at the Cretaceous-Tertiary boundary. Karoo boundary beds, like those in Antarctica and Australia, are redeposited soils, not impact beds with suevite and stishovite. Some of the clasts in South African boundary breccias are calcareous and thus show no evidence of acid rain. Because the Cretaceous–Tertiary boundary extinctions were so much less profound than the Permian–Triassic extinctions, evidence of impact should be more obvious (Retallack et al., 1998). There is some evidence of small impacts, but not one big enough to create the largest extinction in Earth history by itself (Erwin et al., 2002).

Extinction during a transition from aridland to wetland has been suggested for the South African record based on interpretation of most earliest Triassic reptiles as aquatic (Parrington, 1948). There is also evidence for increased flooding from the boundary laminites (Fig. 4) and from a transition from meandering to braided streams (Ward et al., 2000). But *Lystrosaurus*, and many other earliest Triassic creatures, were not aquatic (King and Cluver, 1991; Retallack, 1996; Retallack and Hammer, 1998) and burrowed into well-drained soils (Groenewald, 1991). Furthermore, the magnitude of extinctions worldwide is much greater than would be expected from the magnitude of long-term paleoclimatic change revealed by paleosols. Karoo Permian and Triassic paleosols remained similar in chemical and petrographic composition (Figs. 5 and 6), and paleoclimatic change envisaged here amounted to only one life zone (Figs. 14 and 15), equivalent to going from the alluvial flats of Kyzl Orda, Kazachstan, to the piedmont of Tashkent, Uzbekistan, or from the Karoo desert of Cape Province to the wooded grassland of Orange Free State. This modest paleoclimatic and paleogeographic change is out of all proportion to the magnitude of the extinctions (Retallack, 1995; Looy, 2000; Smith and Ward, 2001). Paleoclimatic and paleogeographic changes in paleosols at the Cretaceous–Tertiary boundary were also modest compared with extinctions (Retallack, 1994), and as in that case, something else is needed to do the damage.

Extinction due to gas emission from the enormous Siberian trap flood basalts has been suggested as a plausible terminal Permian extinction mechanism, mainly because their eruption began at about the same time (Conaghan et al., 1994; Riechow et al., 2002). Even these large eruptions could not release

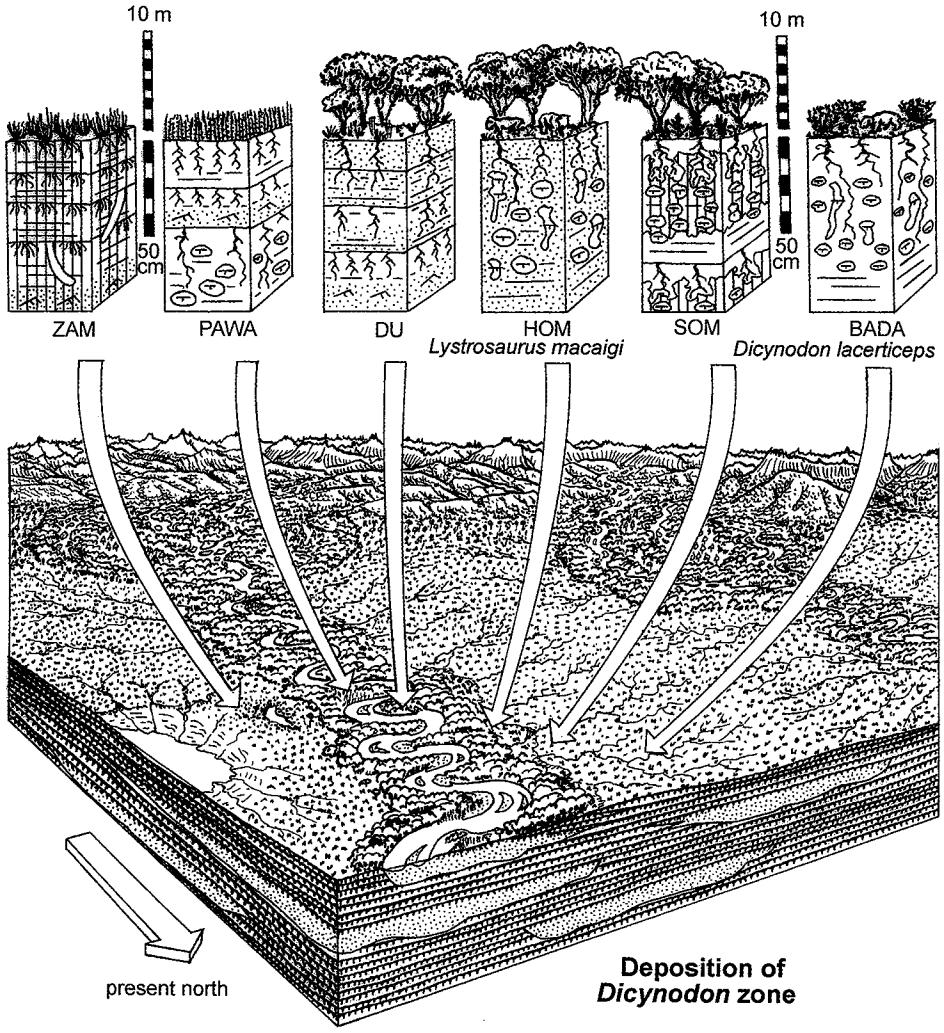

Figure 14. Reconstructed soils and environment near Bethulie during latest Permian.

enough sulfur dioxide, carbon dioxide, and water vapor quickly enough to cause such widespread havoc, and this problem is worsened by recent radiometric dating that reveals a lack of time for the cumulative effect of degassing to reach a critical threshold (Wignall, 2001). Another problem for this theory is the isotopic composition of volcanic carbon dioxide (−7 to −5‰ $\delta^{13}C$), which is isotopically heavier than organic matter (−22 to −24‰ $\delta^{13}C$) and cannot have shifted the isotopic composition of organic matter to values as low as observed (Berner, 2002). In South African soil nodules and therapsid tusks, the carbon isotopic anomaly is marked (MacLeod et al., 2000), as it is throughout the world at the Permian–Triassic boundary (Krull and Retallack, 2000).

Models of death by oceanic anoxia (Isozaki, 1997; Wignall and Twitchett, 1996) are unlikely to affect animals on land, unless there was some kind of massive degassing event of a stratified ocean comparable to the fatal gas outburst from Lake Nyos, Cameroon (Knoll et al., 1996). Even if this model were feasible, given constraints of likely Permian ocean productivity, circulation, and carbon cycling (Hotinski et al., 2001; Berner, 2002), the flow of dense carbon dioxide into the Karoo Basin within a mountain-girt Gondwana supercontinent is unlikely. This model also fails to explain the extreme isotopic depletion seen in carbon isotopic composition of organic matter in South Africa and elsewhere (Krull and Retallack, 2000; MacLeod et al., 2000; de Wit et al. 2002).

A final hypothesis favored here is death by methane from the massive dissociation of methane clathrate reservoirs in permafrost or continental shelves by volcanic eruption, meteorite impact, or submarine landslide (Krull and Retallack, 1999; Krull et al., 2000). This is the only likely explanation for carbon isotopic shifts at the Permian–Triassic boundary of as much as −8‰ $\delta^{13}C$ (Berner, 2002), because carbon with an isotopic value much lower than that of organic matter (−22 to −24‰ $\delta^{13}C$) is required, and methanogenic methane can be as low as −110‰ and is typically −60‰ $\delta^{13}C$ (Whiticar, 2000). Methane released into the atmosphere would have been oxidized to carbon dioxide within 7–24 yr (Khalil et al., 2000). The effects of both methane and carbon dioxide would have been global warming, which would also stabilize higher levels of atmospheric water vapor, another potent greenhouse gas. A postapocalyptic greenhouse is indicated by paleosols studied here and elsewhere (Retallack, 1999a, Retallack and Krull, 1999), by oxygen isotopic studies (Holser et al., 1991; Mii et al., 1997), by stomatal index studies of fossil leaves (Retallack, 2001b), and by modeled equilibration of methane with oceanic and terrestrial carbon reservoirs (Berner, 2002; de Wit et al., 2002). Mass balance modeling studies showing reduced atmospheric oxygenation from 30 volume % to only 12% (Graham et al., 1995; Berner, 2002) agree with stomatal index studies showing earliest Triassic atmospheric CO_2 levels of ~2000 ppmV (Retallack, 2001b), and with the presence of berthierine in Antarctic paleosols, indicating unusually low soil oxygen (Sheldon and Retallack, 2002).

Such an abrupt change in atmospheric composition could kill many marine creatures by acidosis and hypoxia (Knoll et al., 1996) and lead to mass mortality among wetland plants already challenged for oxygen supply to their roots (Retallack et al., 1996; Sheldon and Retallack, 2002). Using algorithms of West (1999), Berner's (2002) proposed dilution of atmospheric oxygen (to 12% by volume) would have brought oxygenation levels comparable to those at the summit of Mt. Everest, currently near the limit for vertebrate life, down to elevations of 4572 m. Oxygenation at elevations of 100–200 m, likely for the Karoo Basin during the Permian–Triassic transition, would have been 420–429 Torr, comparable with an ascent to Zatra Teng Pass near Mount Everest (4943 m) or the South Peak of Kilimanjaro (4983 m) today. Earliest Triassic land vertebrates would have been vulnerable to nausea, headache, hypertension and pulmonary edema, a group of maladies commonly called mountain sickness (Hultgren, 1997). The Permian–Triassic situation would not have been exactly similar to mountain sickness, which is hypobaric hypoxia with alkalosis (Bouverot, 1985), because Permian–Triassic methane would have consumed oxygen in conversion to carbon dioxide to produce normobaric hypoxia with acidosis. Normobar-

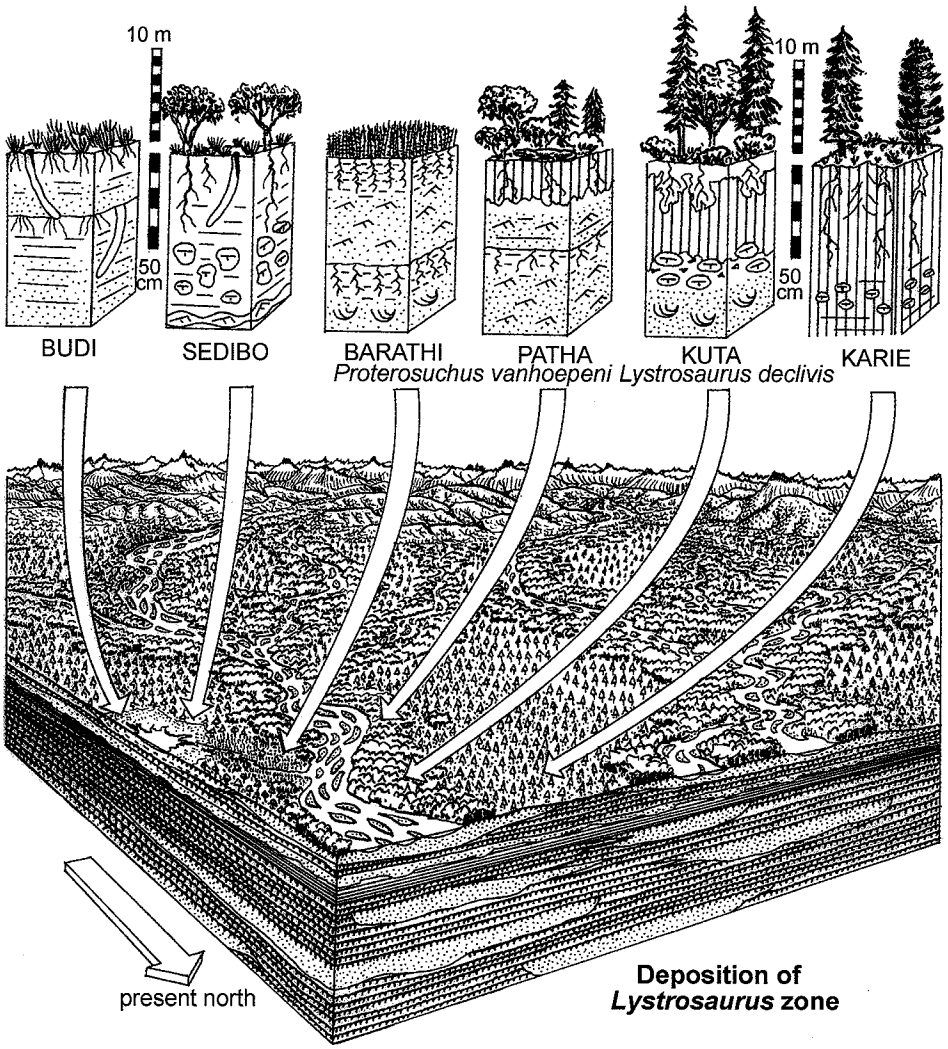

Figure 15. Reconstructed soils and environment near Bethulie during earliest Triassic.

ic hypoxia has been shown to produce similar effects to mountain sickness (Russell and Crook, 1968; Schoene, 1990), and these effects can be exacerbated by hypercapnic acidosis, which also stimulates hyperventilation (Fiddian-Green, 1995; Knoll et al., 1996). Vertebrates have considerable scope to adjust their ventilation rates, and birds are more tolerant of hypoxia than mammals (Scheid, 1990). Hypoxia induces pulmonary vasoconstriction and hypertension and high red blood cell count (Hultgren, 1997), but the principal fossilizable adaptations to hypoxia are large, barrel chests relative to body size and low birth-weight babies at full term (Beall, 1982; Bouverot, 1985; Schoene, 1990). Small, barrel-chested *Lystrosaurus* and *Proterosuchus* in the earliest Triassic offer support to this hypothesis for survival of the terminal Permian atmospheric gas crisis. Greater aerobic scope of earliest Triassic survivors may also be evident in the thickened thoracic, but reduced lumbar ribs of earliest Triassic *Galesaurus* and *Thrinaxodon*, perhaps indicative of a mammalian-style muscular diaphragm (Brink, 1956; MacRae, 1999), and the short snout and internal nares of *Lystrosaurus* and geologically younger dicynodonts, creating a less obstructed upper airway (Cruikshank, 1968; King, 1991). These potential adaptations to hypoxia probably evolved originally in burrowing animals, but were critical to survival of the terminal Permian atmospheric crisis. Further testing of this idea is needed from studies of nasal turbinals, bone vascularization, rib morphology, and spinal chord diameter as adaptations to what may have been an unprecedented atmospheric pollution with hydrocarbons. Nevertheless, we agree with Graham et al. (1997) that the terminal Permian was "a defining moment for amniote physiology and evolution."

ACKNOWLEDGMENTS

We thank R. Buick, T. Evans, N. Ward, and A. Crean for assistance in the field, and N. Sheldon, G. Soreghan, and S. Hasiotis for helpful reviews and discussion. Fieldwork was funded through the University of Washington node of the NASA Astrobiology Institute.

REFERENCES CITED

Alonso-Zarza, A.M., Sanz, M.E., Calvo, J.P., and Estévez, P., 1998, Calcified root cells in Miocene pedogenic carbonates of the Madrid Basin: Evidence for the origin of *Microcodium*: Sedimentary Geology, v. 116, p. 91–97.

Anderson, J.M., 1977, The biostratigraphy of the Permian and Triassic, Part 3, A review of Gondwana Permian palynology, with particular reference to the northern Karoo Basin, South Africa: Botanical Survey of South Africa Memoir, v. 41, 188 p.

Anderson, J.M., and Anderson, H.M., 1985, Palaeoflora of southern Africa: Prodromus of South African megafloras: Devonian to Lower Cretaceous: Rotterdam, A.A. Balkema, 423 p.

Beall, C.M.A., 1982, A comparison of chest morphology in high altitude Asian and Andean populations: Human Biology, v. 54, p. 145–163.

Becker, L., Poreda, R., Hunt, H.G., Bunch, T.E., and Rampino, M., 2001, Impact event at the Permian–Triassic boundary: Evidence from extraterrestrial noble gases in fullerenes: Science, v. 291, p. 1530–1533.

Berner, R.A., 2002, Examination of hypotheses for the Permo-Triassic boundary extinction by carbon cycle modeling: Proceedings of the U.S. Academy of Sciences, v. 99, p. 4172–4177.

Bleek, D.F., 1956, A bushman dictionary: New Haven, Connecticut, American Oriental Society, 773 p.

Botha, B.J.V., and Linström, W., 1978, A note on the stratigraphy of the Beaufort Group in northwestern Natal: Transactions of the Geological Society of South Africa, v. 81, p. 35–50.

Bouverot, P., 1985, Adaptation to altitude hypoxia in vertebrates: Springer, Berlin, 176 p.

Brewer, R., 1976, Fabric and mineral analysis of soils: New York, Krieger, 482 p.

Brink, A.S., 1956, Speculations on some advanced mammalian characteristics in higher mammal-like reptiles: Palaeontographica Africana, v. 4, p. 77–86.

Broili, F., and Schröder, J., 1937, Über *Micropholis* Huxley: Sitzungsberichte der Mathematische-Natürwissenschaftlichen Abteilung der Bayerische Akademie der Wissenschaften zu München, v. 1937, p. 19–38.

Broom, R., 1932, The mammal-like reptiles of South Africa and the origin of mammals: London, Witherby, 376 p.

Brown, J.H., and Lomolino, M.V., 1998, Biogeography: Sunderland, Massachusetts, Sinauer, 691 p.

Busacca, A.J., 1989, Long Quaternary record in eastern Washington, USA: Interpreted from multiple buried paleosols in loess: Geoderma, v. 45, p. 105–122.

Catuneanu, D., and Elango, H.N., 2001, Tectonic control on fluvial styles: The Balfour Formation of the Karoo Basin, South Africa: Sedimentary Geology, v. 140, p. 291–313.

Cluver, M.A., 1971, The cranial morphology of the dicynodont genus *Lystrosaurus*: South African Museum Annals, v. 56, p. 155–274.

Cluver, M.A., and Hotton, N., 1981, The genera *Dicynodon* and *Diictodon* and their bearing on classification of the Dicynodontia (Reptilia, Therapsida): South African Museum Annals, v. 83, p. 1–47.

Conaghan, P.J, Shaw, S.E., and Veevers, J.J., 1994, Sedimentary evidence of the Permian/Triassic global crisis induced by the Siberian hotspot, *in* Embry, A.F, Beauchamp, B., and Glass, D.J., eds., Pangea: Global environments and resources: Canadian Society of Petroleum Geologists Memoir, v. 17, p. 785–795.

Cruickshank, A.R.I., 1968, A comparison of the palates of Permian and Triassic dicynodonts: Palaeontographica Africana, v. 11, p. 23–31.

de Wit, M.J., Ghosh, J.G., de Villiers, S., Rakotosolofo, N., Alexander, J., Tripathi, A., and Looy, C., 2002, Multiple organic carbon isotope reversals across the Permo-Triassic boundary of terrestrial Gondwanan sequences: Clues to extinction patterns and delayed ecosystem recovery: Journal of Geology, v. 110, p. 227–240.

du Toit, A.L., 1939, Geology of South Africa: Edinburgh, Oliver and Boyd, 539 p.

Eberl, D.D., Srodon, J., Kralik, M., Taylor, B.E., and Peterman, Z.E., 1990, Ostwald ripening of clays and metamorphic minerals: Science, v. 248, p. 477.

Egle, S., de Wit, M.J., and Hoernes, S., 1998, Gondwana fluids and subsurface paleohydrology of the Cape Fold Belt and Karoo Basin: Journal of African Earth Sciences, v. 27, p. 63–64.

Erwin, D.H., Bowring, S.A., and Jin, Y.-G., 2002, End-Permian mass-extinctions: A review, *in* Koeberl, C., and MacLeod, K.G., eds., Catastrophic events and mass extinctions: Impacts and beyond: Geological Society of America Special Paper 356, p. 353–383.

Etheridge, R., 1899, On a fern (*Blechnoxylon talbragarense*), with secondary wood, forming a new genus, from the coal measures of the Talbragar district, New South Wales: Records of the Australian Museum, v. 3, p. 135–147.

Fiddian-Green, R., 1995, Gastric intramucosal pH, tissue oxygenation and acid-base balance: British Journal of Anaesthesiology, v. 74, p. 591–606.

Food and Agriculture Organization, 1974, Soil map of the world, Volume I, Legend: Paris, United Nations Educationa, Scientific, and Cultural Organization, 59 p.

Food and Agriculture Organization, 1977, Soil map of the world, Volume VI, Africa: Paris, United Nations Educationa, Scientific, and Cultural Organization, 299 p.

Food and Agriculture Organization, 1978a, Soil map of the world, Volume VIII, North and central Asia: Paris, United Nations Educationa, Scientific, and Cultural Organization, 165 p.

Food and Agriculture Organization, 1978b, Soil map of the world, Volume X, Australasia: Paris, United Nations Educationa, Scientific, and Cultural Organization, 221 p.

Gile, L.H., Hawley, J.W., and Grossman, J.B., 1980, Soils and geomorphology in the Basin and Range area of southern New Mexico: Guidebook New Mexico Bureau of Mines and Mineral Resources, v. 39, 222 p.

Graham, J.B., Dudley, R., Aguilar, N.M., and Gans, C., 1995, Implications of the late Palaeozoic oxygen pulse for physiology and evolution: Nature, v. 375, p. 117–120.

Graham, J.B., Aguilar, N., Dudley, R., and Gans, C., 1997, The late Paleozoic atmosphere and the ecological and evolutionary physiology of tetrapods, *in* Sumida, S.S., and Martin, K.L., eds., Amniote origins: Completing the transition to land: San Diego, Academic Press, p.141–167.

Groenewald, G.H., 1991, Burrow casts from the *Lystrosaurus-Procolophon* assemblage zone: Koedoe, v. 34, p. 13–22.

Groenewald, G.H., and Rust, I.C., 1998, Tectonostratigraphy: An alternative to sequence stratigraphy in the Tarkastad Supergroup, Karoo Basin, South Africa: Journal of African Earth Science, v. 27, p. 95–96.

Groenewald, G.H., Welman, J., and MacEachern, J.A., 2001, Vertebrate burrow complexes from the Early Triassic *Cynognathus* zone (Dreikoppen Formation, Beaufort Group) of the Karoo Basin, South Africa: Palaios, v. 16, p. 148–160.

Hancox, P.J., Brandt, D., Riemold, W.V., Koeberl, C., and Neveling, J., 2002, Permian–Triassic boundary in the northwest Karoo Basin: Development models and the search for evidence of impact: A review, *in* Koeberl, C., and MacLeod, K.G., eds., Catastrophic events and mass extinctions: Impacts and beyond: Geological Society of America Special Paper 356, p. 429–444.

Häntzschel, W., 1975, Treatise of invertebrate paleontology, Part W, Miscellanea, Supplement 1, Trace fossils and problematica: Boulder, Colorado, and Lawrence, Kansas, Geological Society of America and University of Kansas, 269 p.

Haughton, S.H., 1970, Trans-Karoo excursion: Johannesburg, International Gondwana Symposium Guidebook, v. 3, 114 p.

Haycock, C.A., Mason, T.R., and Watkeys, M.K., 1997, Early Triassic palaeoenvironments in the eastern Karoo foreland basin, South Africa: Journal of African Earth Sciences, v. 24, 79–94.

Hiller, N., and Stavrakis, N., 1984, Permo-Triassic fluvial systems in the southeastern Karoo Basin, South Africa: Palaeogeography, Palaeoclimatology, Palaeoecology, v. 45, p. 1–21.

Holser, W.T., Schönlaub, H.P., and Magaritz, M., 1991, The Permian–Triassic of the Gartnerkofel core (Carnic Alps, Austria): Synthesis and conclusions, *in* Holser, W.T., and Schönlaub, H.P., eds., The Permian–Triassic boundary in the Carnic Alps of Austria (Gartnerkofel region): Vienna, Abhandlungen Bundesanstalt Autriche, v. 45, p. 213–232.

Horner, T.C., and Krissek, L.A., 1991, Contributions of sedimentologic thermal alteration and organic carbon to paleoenvironmental interpretation of fine-grained Permian clastics from the Beardmore Glacier region, Antarctica, *in* Elliot, D.H., ed., Contributions to Antarctic Research: American Geophysical Union Research Series, v. 53, p. 33–65.

Hotinski, R.M., Bice, K.L., Kump, L.R., Najjar, R.G., and Arthur, M.A., 2001, Ocean stagnation and end-Permian anoxia: Geology, v. 29, p. 7–10.

Hotton, N., Olson, E.C., and Beerbower, R., 1997, Amniote origins and the discovery of herbivory, *in* Sumida, S.S., and Martin, K.L., eds., Amniote origins: Completing the transition to land: San Diego, Academic Press, p. 207–264.

Hultgren, H., 1997, High altitude medicine: Stanford, Hultgren, 550 p.

Isozaki, Y., 1997, Permo-Triassic boundary superanoxia and stratified superocean: Records from lost deep sea: Science, v. 276, p. 235–238.

Johnson, M.R., 1991, Sandstone petrography, provenance and plate tectonic setting in Gondwana context of the Cape-Karoo Basin: South African Journal of Geology, v. 94, p. 137–154.

Kemp, T.S., 1986, The skeleton of a baurioid therocephalian therapsid from the Lower Triassic (*Lystrosaurus* zone) of South Africa: Journal of Vertebrate Paleontology, v. 6, p. 215–232.

Keyser, A.W., 1968, Some indications of arid climate during the deposition of the Beaufort Series: Geological Survey of South Africa Annals, v. 5, p. 77–78.

Khalil, M.A.K., Shearer, M.J., and Rasmussen, R.A., 2000, Methane sinks, distribution and trends, *in* Khalil, M.A.K., ed., Atmospheric methane: Berlin, Springer, p. 86–97.

King, G.M., 1981, The functional anatomy of a Permian dicynodont: Royal Society of London, Philosophical Transactions, v. B291, p. 243–322.

King, G.M., 1991, The Dicynodonts: A study in paleobiology: London, Chapman and Hall, 233 p.

King, G.M., 1993, Species longevity and generic diversity in dicynodont mammal-like reptiles: Palaeogrography, Palaeoclimatology, Palaeoecology, v. 102, p. 321–332.

King, G.M., and Cluver, M.A., 1991, The aquatic Lystrosaurus: An alternative lifestyle: Historical Biology, v. 4, p. 232–341.

Kitching, J.W., 1977, The distribution of Karoo vertebrate fauna: Bernard Price Institute for Palaeontological Research Memoir, v. 1, 131 p.

Klappa, C.F., 1978, Biolithogenesis of *Microcodium*: Elucidation: Sedimentology, v. 25, p. 489–522.

Knoll, A.H., Bambach, R.K, Canfield, D.E., and Grotzinger, J.F., 1996, Comparative Earth history and the late Permian mass extinction: Science, v. 273, p. 452–457.

Knystautas, A., 1987, The natural history of the U.S.S.R.: London, Century, 224 p.

Krassilov, V.A., Afonin, S.A., and Baranova, S.S., 1999, *Tympanicysta* and the terminal Permian events: Permophiles, v. 35, p. 16–17.

Krull, E.S., and Retallack, G.J., 2000, $\delta^{13}C_{org}$ depth profiles from paleosols across the Permian–Triassic boundary: Evidence for methane release: Geological Society of America Bulletin, v. 112, p. 1459–1472.

Krull, E.S., Retallack, G.J., Campbell, H.J., and Lyon, G.L., 2000, $\delta^{13}C_{org}$ chemostratigraphy of the Permian–Triassic boundary in the Maitai Group, New Zealand: Evidence for high latitude methane release: New Zealand Journal of Geology and Geophysics, v. 43, p. 21–32.

Lawrence, P.F., 1984, The centipedes and millipedes of southern Africa: A guide: Cape Town, A.A. Balkema, 148 p.

Lavrenko, E.M., and Karamysheva, Z.V., 1993, Steppes of the former Soviet Union and Mongolia: *in* Coupland, R.T., ed., Natural grasslands: Ecosystems of the world: Amsterdam, Elsevier, v. 8B, p. 3–59.

Looy, C.V., 2000, The Permian–Triassic biotic crisis: Collapse and recovery of terrestrial ecosystems: Utrecht, Laboratory of Palaeobotany and Palynology Contributions, v. 13, 114 p.

Looy, C.V., Twitchett, R.J., Dilcher, D.L., van Kojnijnenberg-van Cittert, J.H.A., and Visscher, H., 2001, Life in the end-Permian dead zone: U.S. National Academy of Sciences Proceedings, v. 98, p. 7879–7883.

Mack, G.H., and James, W.C., 1994, Paleoclimate and global distribution of paleosols: Journal of Geology, v. 102, p. 360–372.

Mack, G.H., James, W.C., and Monger, H.C., 1993, Classification of paleosols: Geological Society of America Bulletin, v. 105, p. 129–136.

MacLeod, K.G., Smith, R.M.H., Koch, P.L., and Ward, P.G., 2000, Timing of mammal-like reptile extinctions across the Permian–Triassic boundary in South Africa: Geology, v. 24, p. 227–230.

MacRae, C., 1999, Life etched in stone: Fossils of South Africa: Johannesburg, Geological Society of South Africa, 305 p.

Mader, D., 1990, Palaeoecology of the flora in Buntsandstein and Keuper in the Triassic of Middle Europe: Hannover, G. Fischer, 1687 p.

Maisch, M.W., 2002, A new basal lystrosaurid dicynodont from the upper Permian of South Africa: Palaeontology, v. 45, p. 343–359.

McFadden, L.D., and Tinsley, J.C., 1985, Rate and depth of pedogenic carbonate accumulation in soils: Formulation and testing of a compartmnent model, *in* Weide, D.L., ed., Soils and Quaternary geology of the southwestern United States: Geological Society of America Special Paper 203, p. 23–41.

Mii, H.-S., Grossman, E.L., and Yancey, T.E., 1997, Stable-carbon and oxygen isotopic composition of west Spitzbergen: Global change or diagenetic artifact?: Geology, v. 25, p. 227–230.

Molnar, P., and England, P., 1990, Late Cenozoic uplift of mountain ranges and global cooling: Chicken or egg?: Nature, v. 246, p. 29–34.

Morante, R., 1996, Permian and Early Triassic isotopic records of carbon and strontium in Australia and a scenario of events about the Permian–Triassic boundary: Historical Biology, v. 11, p. 289–310.

Müller, M.J., 1982, Selected climatic data for a global set of standard stations for vegetation science: The Hague, Junk, 306 p.

Parrington, F.R., 1948, Labyrinthodonts from South Africa: Proceedings of the Zoological Society of London, v. 1.118, p. 426–445.

Pehl, C.W., Kirschvink, J.L., and Ward, P.D., 2001, Towards a magnetostratigraphy of the terrestrial Permian–Triassic boundary: Geological Society of America Abstracts with Programs, v. 33, no. 6, p. 390.

Plumstead, E.P., 1969, Three thousand million years of plant life in Africa: Geological Society of South Africa Alex L. du Toit Memorial Lecture, v. 11, 72 p.

Ratcliffe, B.C., and Fagerstrom, J.A., 1980, Invertebrate lebensspuren of Holocene floodplains: Their morphology, origin and paleoecological significance: Journal of Paleontology, v. 54, p. 614–630.

Rayner, R.J., 1992, *Phyllotheca*; the pastures of the Late Permian: Palaeogeography, Palaeoclimatology, Palaeoecology, v. 92, p. 31–40.

Riechow, M.K., Saunders, A.D., White, R.V., Pringle, M.S., Mukhamedov, A.I., Medvedev, A.I., and Kirda, N.P., 2002, $^{40}Ar/^{39}Ar$ dates from west Siberian basin: Siberian flood basalt province doubled: Science, v. 296, p. 1846–1849.

Renne, P.R., Zheng, Z.C., Richards, M.A., Black, M.T., and Basu, A.R., 1995, Synchrony and causal relations between Permian–Triassic boundary crisis and Siberian flood volcanism: Science, v. 269, p. 1413–1416.

Retallack, G.J., 1983, Late Eocene and Oligocene paleosols from Badlands National Park, South Dakota: Geological Society of America Special Paper 193, 82 p.
Retallack, G.J., 1991a, Untangling the effects of burial alteration and ancient soil formation: Annual Reviews of Earth and Planetary Sciences, v. 19, p. 183–206.
Retallack, G.J., 1991b, Miocene paleosols and ape habitats of Pakistan and Kenya: New York, Oxford University Press, 346 p.
Retallack, G.J., 1994, A pedotype approach to latest Cretaceous and earliest Tertiary paleosols in eastern Montana: Geological Society of America Bulletin, v. 106, p. 1377–1397.
Retallack, G.J., 1995, Permian–Triassic life crisis on land: Science, v. 267, p. 77–80.
Retallack, G.J., 1996, Early Triassic therapsid footprints from the Sydney Basin, Australia: Alcheringa, v. 20, p. 301–314.
Retallack, G.J., 1997a, A colour guide to paleosols: Chichester, England, Wiley, 175 p.
Retallack, G.J., 1997b, Earliest Triassic origin of *Isoetes* and quillwort evolutionary radiation: Journal of Paleontology, v. 71, p. 500–521.
Retallack, G.J., 1997c, Dinosaurs and dirt, *in* Wolberg, D., and Stump, E., eds., Dinofest: Philadelphia, Academy of Natural Sciences, p. 345–359.
Retallack, G.J., 1998, Fossil soils and completeness of the rock and fossil record, *in* Donovan, S.K., and Paul, C.R.C., eds., The adequacy of the fossil record: Chichester, Wiley, p. 132–163.
Retallack, G.J., 1999a, Postapocalyptic greenhouse revealed by earliest Triassic paleosols in the Sydney Basin, Australia: Geological Society of America Bulletin, v. 111, p. 52–70.
Retallack, G.J., 1999b, A Jurassic prehnite vein intruding the Permian–Triassic boundary at Graphite Peak, Antarctica: U.S. Antarctic Journal, v. 30, p. 5–7.
Retallack, G.J., 2000, Depth to pedogenic carbonate as a paleoprecipitation indicator? Comment: Geology, v. 28, p. 572–573.
Retallack, G.J., 2001a, *Scoyenia* burrows from Ordovician palaeosols of the Juniata Formation in Pennsylvania: Palaeontology, v. 44, p. 209–235.
Retallack, G.J., 2001b, A 300-million-year record of atmospheric carbon dioxide from fossil plant cuticles: Nature, v. 411, p. 287–290.
Retallack, G.J., 2002a, Carbon dioxide and climate over the past 300 Myr: Royal Society of London Philosophical Transactions, v. A360, p. 659–674.
Retallack, G.J., 2002b, *Lepidopteris callipteroides* (Carpentier) comb. nov., an earliest Triassic seed fern of the Sydney Basin, southeastern Australia: Alcheringa, v. 26, p. 475–500.
Retallack, G.J., and Hammer, W.R., 1998, Paleoenvironment of the Triassic therapsid *Lystrosaurus* in the central Transantarctic Mountains, Antarctica: U.S. Antarctic Journal, v. 31, p. 33–35.
Retallack, G.J., and Krull, E.S., 1999, Landscape ecological shift at the Permian–Triassic boundary in Antarctica: Australian Journal of Earth Sciences, v. 46, p. 785–812.
Retallack, G.J., Veevers, J.J., and Morante, R., 1996, Global coal gap between Late Permian extinction and Middle Triassic recovery of peat-forming plants: Geological Society of America Bulletin, v. 108, p. 195–207.
Retallack, G.J., Seyedolali, A., Krull, E.S., Holser, W.T., Ambers, C.P., and Kyte, F.T., 1998, Search for evidence of impact at the Permian–Triassic boundary in Antarctica and Australia: Geology, v. 26, p. 979–982.
Royer, D.L., 1999, Depth to pedogenic carbonate as a paleoprecipitation indicator?: Geology, v. 27, p. 1123–1126.
Rubidge, B.S., ed., 1995, Biostratigraphy of the Beaufort Group (Karoo Supergroup): South African Committee for Stratigraphy Biostratigraphic Series, v. 1, 45 p.
Russell, J.A., and Crook, L., 1968, Comparison of metabolic responses of rats produced by two methods: American Journal of Physiology, v. 214, p. 111–116.
Scheid, P., 1990, Avian respiratory system and gas exchange; *in* Sutton, J.P., Coates, G., and Remmers, J.E., eds., Hypoxia: the Adaptations: Toronto, B.C. Decker, p. 4–8.
Schoene, R.B., 1990, High altitude pulmonary edema: Search for a mechanism; *in* Sutton, J.P., Coates, G., and Remmers, J.E., eds., Hypoxia: the Adaptations: Toronto, B.C. Decker, p. 246–259.
Sehgal, J.L., Sys, C., and Bhumbla, D.R., 1968, A climatic soil sequence from the Thar Desert to the Himalayan Mountains in Punjab (India): Pedologie, v. 20, p. 59–72.
Sephton, M.A., Looy, C.V., Veefkind, R.J., Brinkhuis, H., De Leeuw, J.W., and Visscher, H.J., 2002, Syncrhonous record of $\delta^{13}C$ shifts in the oceans and atmosphere at the end of the Permian, *in* Koeberl, C., and MacLeod, K.G., eds., Catastrophic events and mass extinctions: Impacts and beyond: Geological Society of America Special Paper 356, p. 455–462.
Sheldon, N.D., and Retallack, G.J., 2001, Equation for compaction of paleosols due to burial: Geology, v. 29, p. 247–250.
Sheldon, N.D., and Retallack, G.J., 2002, Low oxygen in earliest Triassic soils: Geology, v. 30, p. 919–922.
Sheldon, N.D., Retallack, G.J., and Tanaka, S., 2002, Geochemical climofunctions from North American soils and application to paleosols across the Eocene–Oligocene boundary in Oregon: Journal of Geology, v. 110, p. 687–696.
Smith, R.M.H., 1987, Helical burrow casts of therapsid origin from the Beaufort Group (Permian) of South Africa: Palaeogeography, Palaeoclimatology, Palaeoecology, v. 60, p. 155–170.
Smith, R.M.H., 1990, Alluvial paleosols and pedofacies sequences in the Permian, Lower Beaufort of the southwestern Karoo Basin, South Africa: Journal of Sedimentary Petrology, v. 60, p. 258–276.
Smith, R.M.H., 1993a, Vertebrate taphonomy of Late Permian floodplain deposits in the southwestern Karoo Basin of South Africa: Palaios, v. 8, p. 45–67.
Smith, R.M.H., 1993b, Sedimentology and ichnology of floodplain paleosurfaces in the Beaufort Group (Late Permian), Karoo sequence, South Africa: Palaios, v. 8, p. 339–357.
Smith, R.M.H., 1995, Changing fluvial environments across the Permian–Triassic boundary in the Karoo Basin, South Africa, and possible causes of the extinctions: Palaeogeography, Palaeoclimatology, Palaeoecology, v. 117, p. 81–104.
Smith, R.M.H., and MacLeod, K.G., 1998, Sedimentology and carbon isotope stratigraphy across the Permian–Triassic boundary in the Karoo Basin, South Africa: Journal of African Earth Sciences, v. 27, p. 185–186.
Smith, R.M.H., and Ward, P.D., 2001, Pattern of vertebrate extinctions across an event bed at the Permian–Triassic boundary in the Karoo Basin of South Africa: Geology, v. 29, p. 1147–1150.
Soil Survey Staff, 1999, Keys to soil taxonomy: Blacksburg, Virginia, Pocahontas Press, 600 p.
Soil Classification Working Group, 1991, Soil classification: A taxonomic system for South Africa: Agriculture Natural Resources South Africa Memoir, v. 15, 257 p.
Stace, H.C.T., Hubble, G.D., Brewer, R., Northcote, K.H., Sleeman, J.R., Mulcahy, M.J., and Hallsworth, E.G., 1968, A handbook of Australian soils: Adelaide, Rellim, 429 p.
Stapleton, R.P., 1978, Microflora from a possible Permo–Triassic transition in South Africa: Review of Palaeobotany and Palynology, v. 25, p. 253–258.
Sarkar, A., Yoshioka, H., Ebihara, M., and Naraoka, H., 2003, Geochemical and organic carbon isotope studies across the continental Permo–Triassic boundary of Raniganj Basin, eastern India: Palaeogeography, Palaeoclimatology, Palaeoecology, v. 191, p. 1–14.
Steiner, M.B., Eshet, Y., Rampino, M.R., and Schwindt, D.M., 2001, Simultaneous Permo-Triassic boundary marine and terrestrial mass extinctions: The global fungal spike discovered in the Karoo Supergroup (South Africa): Geological Society of America Abstracts with Programs, v. 33, no. 6, p. 201.
Suttner, L.J., and Dutta, P.K., 1986, Alluvial sandstone composition and paleoclimate. I Framework mineralogy: Journal of Sedimentary Petrology, v. 56, p. 329–345.
Twitchett, R.J., Looy, C.V., Morante, R., Visscher, H., and Wignall, P.B., 2001, Rapid collapse of marine and terrestrial ecosystems during the end-Permian biotic crisis: Geology, v. 29, p. 351–354.
van der Westhuizen, W.A., Loock, J.C., and Strydom, D., 1981, Halite imprints in the Whitehill Formation, Ecca Group, Carnarvon district: Geological Survey of South Africa Annals, v. 15, p. 43–46.
Veevers, J.J., Cole, D.J., and Cowan, E.J., 1994, Southern Africa: Karoo Basin and Cape Fold Belt, *in* Veevers, J.J., and Powell, C.M^{c}.A., eds., Permian–Triassic Pangean basins along the Panthalassan margin of Gondwanaland: Geological Society of America Memoir, v. 184, p. 223–279.
Visscher, H., Brinkhuis, K., Dilcher, D.L., Elsik, W.C., Eshet, Y., Looy, C., Rampino, M.R., and Traverse, A., 1996, The terminal Paleozoic fungal event: Evidence of terrestrial ecosystem destabilization and collapse: National Academy of Sciences United States Proceedings, v. 93, p. 2135–2158.
Walton, J., 1925, On some South African fossil woods: Annals of the South African Museum, v. 22, p. 1–26.
Walton, J., 1936, On the factors which influence the external form of fossil plants: With descriptions of some species of the Paleozoic equisetalean genus *Annularia* Sternberg: Philosophical Transactions of the Royal Society of London, v. B226, p. 219–237.
Wang, Z.-Q., 1996, Recovery of vegetation from the terminal Permian mass extinction in North China: Review of Palaeobotany and Palynology, v. 9, p. 121–124.
Ward, P.D., Montgomery, D.R., and Smith, R.M.H., 2000, Altered river morphology in South Africa related to the Permian–Triassic extinction: Science, v. 289, p. 1740–1743.
Warren, E., 1912, On some specimens of fossil woods in the Natal Museum: Annals of the Natal Museum, v. 2, p. 345–380.
Watson, D.M.S., 1960, The anomodont skeleton: Zoological Society of London Transactions, v. 29, p. 131–205.
West, J.B., 1999, Recent advances in human physiology at extreme altitude, *in* Roach, R.C., Wagner, P.D., and Hackett, P.H., eds., Hypoxia: Into the Next Millenium: New York, Plenum, p. 257–296.
White, M.E., 1986, The greening of Gondwana: Reed, Frenchs Forest, Australia, 256 p.
Whittaker, R.H., and Woodwell, G.M., 1968, Dimension and production relations of trees and shrubs in the Brookhaven forest, New York: Journal of Ecology, v. 56, p. 1–25.
Wignall, P.B., 2001, Large igneous provinces and mass extinctions: Earth Science Reviews, v. 53, p. 1–33.
Wignall, P.B, and Twitchett, R.J., 1996, Oceanic anoxia and the terminal Permian mass extinction: Science, v. 272, p. 1155–1158.
Whiticar, M.J., 2000, Can stable isotopes and global budgets be used to constrain atmospheric methane budgets? *in* Khalil, M.A.K., ed., Atmospheric methane: Berlin, Springer, p. 63–85.
Yang, Z.Y., Sheng, J.Z., and Yin, H.F., 1996, The Permian–Triassic boundary: Global stratotype section and point (GSSP): Episodes, v. 18, p. 49–53.
Zawada, P.K., 1984, Preliminary geochemical investigation of Ecca and Beaufort Group mudrocks in the Fauresmith area, Orange Free State: Geological Survey of South Africa Annals, v. 18, p. 53–65.
Zawada, P.K., 1988, The stratigraphy and sedimentology of the Ecca and Beaufort Groups in the Fauresmith area, southwestern Orange Free State: Geological Survey of South Africa Bulletin, v. 90, 48 p.
Zhou, Y.-Q., and Chai, C.-F., 1991, The discovery of shocked quartz and stishovite in the Permian/Triassic boundary clay of Huangshi, China: Meteoritics, v. 26, p. 413.
Zohary, M., 1973, Geobotanical foundations of the Middle East: Stuttgart, Gustav Fischer, 738 p.

MANUSCRIPT RECEIVED BY THE SOCIETY 10 JULY 2002
REVISED MANUSCRIPT RECEIVED 30 MARCH 2003
MANUSCRIPT ACCEPTED 1 APRIL 2003

Printed in the USA